

THESIS

2000



LIBRARY

Michigan State University

# PLACE IN RETURN BOX to remove this checkout from your record. TO AVOID FINES return on or before date due. MAY BE RECALLED with earlier due date if requested.

DATE DUE	DATE DUE	DATE DUE

11/00 c/CIRC/DateDue.p65-p.14

# MODELING THE SOLIDIFICATION OF SEMICRYSTALLINE POLYMERS

By

 $Durgesh\ Rege$ 

#### A THESIS

Submitted to
Michigan State University
in partial fulfillment of the requirements
for the degree of

MASTER OF SCIENCE

Mechanical Engineering

#### ABSTRACT

# MODELING THE SOLIDIFICATION OF SEMICRYSTALLINE POLYMERS

Bv

#### Durgesh Rege

Modeling the solidification of semicrystalline polymers is considered in this work. This is done to study the possibility of fabricating in-situ polymer/polymer composites using directional solidification. With this technique, a thermal gradient is applied to induce orientation of the crystals in a polymer blend composed of a semicrystalline polymer and an amorphous polymer. A numerical model is first developed based on the Eikonal equation to track the interfaces of the developing spherulites. The travel times of the growing spherulites can be computed rapidly using a simple finitedifference scheme. Isothermal solidification with instantaneous nucleation is considered for two-dimensional crystallization processes. The model correctly accounts for the growth of single or multiple spherulites and their impingement without special treatment. The model also accounts for the growth of spherulites in the presence of obstacles such as fibers or the growth of spherulites in the presence of a thermal gradient. Theoretical work is also performed to identify the thermal conditions that favor steady growth and suppress excessive nucleation ahead of the growing interface. Furthermore, stability issues are addressed to estimate whether a solid/liquid interface will be planar under directional solidification conditions.

		· ·
		1

To my family

#### ACKNOWLEDGMENTS

I would like to express my deepest appreciation to the following people for having made the completion of this thesis possible:

To my advisor Dr. Andre Benard, for his insight, guidance and invaluable assistance, without which this thesis would not have been possible. His dedication to the subject and personal integrity have served as an example and an inspiration to me.

To my other committee members, Dr. McGrath and Dr. Somerton for their valuable suggestions and comments.

To Research Excellence Funds and the Composite Materials and Structures Center for providing financial support for two years.

To all my other instructors at MSU, for their skillful instruction in the classroom, but more importantly, for their constant encouragement and friendship.

To my friends, for having made my stay here the memorable experience that it has been.

And to my family, for years of support, patience and understanding.

#### TABLE OF CONTENTS

LIST OF FIGURES	vii
LIST OF TABLES	ix
1 Introduction	1
2 Crystallization in the Presence of a Temperate	ure Gradient and So-
lute	9
2.1 Introduction	9
2.2 Nucleation of Spherulites	10
2.3 Growth of spherulites	15
2.4 Directional Solidification	
2.4.1 Problem Formulation and Calculations	21
2.4.2 Results and Discussion	
3 Morphological Instability of a Planar Interface	e during Directional
Solidification	25
3.1 Introduction	25
3.2 Computation of the Solute Concentration Ahead of	a Wavy Interface 27
3.3 Analysis of morphological instability	
4 Using the Eikonal equation to Model the Phase	Change in Semicrys-
talline Polymers and their Composites	34
4.1 Introduction	
4.2 Factors influencing the spherulitic morphology	
4.3 Previous work done in numerical modeling	
4.4 Basis of the simulation	<b>3</b> 9
4.5 Vidale's scheme	43
4.6 Sethian's approach	47
4.7 Implementation of the scheme	50
4.8 Results and Discussion	51
4.8.1 Spherulitic Growth in a Neat Polymer	51
4.8.2 Spherulitic Growth in the Presence of Obstacles	
4.8.3 Spherulitic Growth in the Presence of a Tempera	ture Gradient 58
4.9 Conclusions	
5 Summary and Conclusions	61

6	Suggestions for Future Work	(
ΑF	PPENDICES	(
A	C code based on Sethian's approach	(
	Matlab program for simulations based on Vidale's scheme	
B.1	l mex.m	
B.2	2 chmi.m	
B.3	B middle.m	
B.4	4 corner.m	

## LIST OF FIGURES

1.1	Micrography of a spherulite taken in the laboratory of Dr. McGrath (Courtesy of Eric Kaiser)
2.1	Nucleation rate as a function of temperature of crystallization
2.2	New nucleation rate as a function of temperature of crystallization
2.3	Growth rate (m/sec) as a function of temperature of crystallization(°C) for isotactic polypropylene
2.4	Schematic for the directional solidification apparatus used
2.5	Temperature gradient (°C/cm) as a function of velocity of growth front(m/sec)for isotactic polypropylene
3.1	Solute concentration ahead of the planar solid/liquid interface
3.2	Solute concentration ahead of the perturbed solid/liquid interface (x nd y distance is in m)
3.3	Stability criterion for isotactic polypropylene
4.1	Initial concept (now deemed erroneous) used in modeling of a spherulite nucleating at N and growing around a circular obstacle
4.2	A schematic diagram of the shadow behind the circular obstacle with center at M
4.3	Illustration of a propagating circle and the corresponding zero level set .
4.4	A schematic depiction of a source point A (nucleus) and its neighbors in the ring
4.5	A 2-D grid showing the numerical calculation of travel times
4.6	An illustration of the sequence of solution of one edge of the ring
4.7	Flowchart for Sethian's method
4.8	Front position of a spherulite at different times while growing in an uniform temperature field (Grid size = 100×100 microns and the times are in microns/sec)
4.9	Shape of two spherulites at different times illustrating impingement and subsequent growth (Grid size = 100×100 microns and the times are in microns/sec)
4.10	Impingement of multiple spherulites with randomly located nuclei shown at different instants (Grid size = 100×100 microns and the times are in microns/sec)

4.11	Growth of a spherulite in the presence of a rectangular obstacle shown	
	at different times (Grid size = 100×100 microns and the times are in	
	microns/sec)	56
4.12	Spherulitic growth in presence of multiple obstacles shown at different	
	times (Grid size = 100×100 microns and the times are in microns/sec)	57
4.13	Spherulitic growth in the presence of a temperature gradient shown at	
	different times (Grid size = 100×100 microns, times are in microns/sec	
	and $dT/dx = 10^{4} \text{ G/m}$ )	59

## LIST OF TABLES

2.1	Values of the parameters from data published in Prog. Polym. Sci	23
3.1	Assumed values of various parameters	29

# Chapter 1

# Introduction

Among the multitude of materials available today, there exists a class of materials called polymers. Their range of behavior and molecular configurations are so wide that further sub-divisions are inevitably made. In fact so different are their properties and processing requirements that they form the basis of an industry of their own. Polymers, or plastics as they are commonly referred to when man-made, are a relatively new class of materials. Although first developed toward the end of the nineteenth century, synthetic polymers found major practical uses only after World War II mainly due to cut-off of key natural raw materials. Since then the polymer industry is advancing in technology and volume growth and today is one of the most prosperous industries in the field of materials.

Polymers can be distinguished broadly as thermoplastics or thermosets. Thermoplastics are fully polymerised in their raw state and there is essentially no chemical reaction involved in processing. Application of heat results in softening or melting of these materials at which time the material flows and can be formed or molded into the desired shape. This cycle is reversible and allows the reuse of a polymer in various products. Thermosets on the other hand are not fully polymerised in their raw state. They contain a partially polymerised polymer and a substance called a

catalyst. Application of heat and pressure first causes softening and after several minutes the catalyst breaks down and initiates a chemical reaction which completes the polymerization or "curing" of the polymer.

In this work the class of polymers under consideration is thermoplastics. It will actually be a study of thermoplastic polymer blends. The growth of this blend technology has significantly increased in the last two decades for the obvious reason that customized property profiles are not always available from a pure polymer at the desired cost. It is always more time and cost efficient to modify the existing polymer product through blending and alloying.

The microstructure of thermoplastic polymer products is one of the dominant factors that determine their chemical and mechanical properties. The properties of semicrystalline polymers, in particular, are generally more sensitive than other materials to the processing conditions as their microstructure can be influenced dramatically by the processing method chosen.

The microstructure of these semicrystalline materials is generally defined by the growth of crystalline entities called spherulites. The growth and morphology of spherulites arising in semicrystalline polymers have been studied extensively over the past thirty years. A brief literature review is outlined in the next section.

Some of the earliest work done on the microstructure of semicrystalline polymers was by Keith and Padden [1, 2] at the Bell Telephone Laboratories. Their work gave the first insight into the causes of the spherulitic morphology observed in polymers. In most examples of crystal growth, a primary nucleus grows into a crystallite having a discrete crystallographic orientation. In spherulites however, primary nuclei also initiate the formation of polycrystalline aggregates with no crystallographic orientation, which are more or less radially symmetric. It was also discovered that all high density polymers crystallize from the melt or from concentrated solution with a

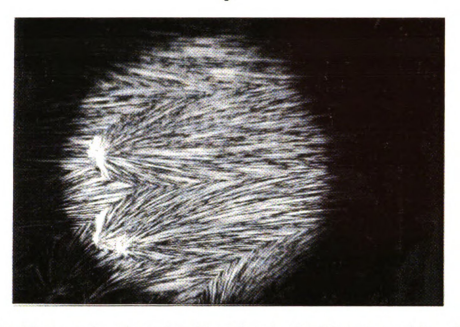


Figure 1.1: Micrography of a spherulite taken in the laboratory of Dr. McGrath (Courtesy of Eric Kaiser)

spherulitic habit and hence there has been a significant interest in this field. It was also noticed that there are similarities between spherulitic crystallization in a wide range of substances - organic and inorganic, polymeric and nonpolymeric etc. These similarities were so pronounced that they could scarcely be coincidental. Hence a conclusion was reached that all of the mechanisms of spherulitic crystallization could be accounted for on a unified basis.

Keith and Padden[1] concluded that spherulitic crystallization is a characteristic property of all systems in which two specific requirements are satisfied. First, conditions should be favorable for the formation of crystals with a fibrous habit and secondly that the fibers formed must be capable of noncrystallographic "small angle branching". Individual fibers branch and develop into sheaves followed by further branching and ultimately resulting in spherulitic growth. They made a detailed study of all the significant physical factors which are responsible for this spherulitic crystallization. One of the first facts observed was that the growth of a spherulite at constant radial rate represents a steady state process and not an equilibrium one. The next most important observation was the vital role played by the impurities in promoting a fibrous habit in spherulitic crystallization. An impurity rich layer of thickness  $\delta$ = D/G, where D is the diffusion coefficient for impurity in the melt, and G is the radial growth rate of a spherulite, which is formed in the liquid at the interface plays a major role in inducing a fibrous habit in these melts. Regarding, "small angle branching", screw dislocations or local temperature gradients were thought to be the cause for fibers to branch but the noncrystallographic nature of this branching could not be explained. This feature was attributed to sufficiently small diffusion coefficients which ensure that values of  $\delta$  are small enough for branching to be predominantly noncrystallographic. In fact it was inferred that the frequency of noncrystallographic branching varies inversely with the magnitude of  $\delta$ . This study was a milestone in the progress of polymer engineering. To summarize the observations made by Keith and Padden [1], it could be said that: a spherulite can be regarded as a particular type of saturation dendrite which rejects impurities which get trapped between the fibers. The melt is extremely viscous and hence the growth of fibrils is fast in comparison with the rate at which impurities can diffuse away. Hence kinetics of radial growth are linear and the process is controlled by nucleation rather than mass diffusion.

However this theory proposed by Keith and Padden[1, 2] was challenged by Bassett et al.[3]. Their studies concluded that solutal effects are not the fundamental reason for the spherulitic morphology as proposed by Keith and Padden. They observed certain spherultic microstructures without the 'fibers' or cellular habits. Also, the solute layer of thickness  $\delta$  does not always correlate with lamellar width as discussed earlier. Hence it was proved that kinetic effects and crystallization temperature also played a major role in the formation of spherulites and solute diffusion was not the only cause of the spherulitic morphology.

Extensive analytical modeling has been carried out over the past fifty years to de-

scribe the crystallization of polymers under isothermal and non-isothermal conditions. The earliest of the models predicted the evolution of the crystallinity as a function of temperature. This was followed by modeling the spherulitic growth in polymers based on the concepts of metallurgy. These models accounted for the heat and mass balance as well as the interfacial kinetics. Avrami[4] followed by many others developed analytical models to address the important aspects such as nucleation. The theory of growth of polymer crystals (the lamellae of a spherulite) was originally developed by Hoffman and Lauritzen[5]. Further issues such as growth of multiple spherulites and the inevitable impingement between them was studied by Avrami who introduced a correction factor that related the volume of spherulites growing freely in an infinite medium to the actual volume of impinging spherulites. However all these models are limited in their applications. They cannot predict growth morphology in polymer composites. They cannot account for phenomena such as growth of spherulites in the presence of one or more obstacles or 'fibers' as well as in the presence of a thermal gradient. Also, they fail to address issues at the microscopic level such as the stability of the solid/liquid interface.

Landmark work was done by Mullins and Sekerka [6, 7] in 1963 when they established the stability criterion for the solid-liquid interface. They theoretically investigated the stability of the shape of a moving planar liquid-solid interface during the unidirectional freezing of a dilute binary alloy by calculating the time dependence of the amplitude of a sinusoidal perturbation of infinitesimal amplitude introduced into the planar shape. They deduced the stability criterion which was expressed in terms of growth parameters. Instability occurs if any arbitrary perturbation grows and stability occurs if all components decay. Using parameters such as surface tension, the conditions of phase of equilibria, temperature gradients on both sides of the interface and the solute concentration gradient, they derived the conditions of stability as a

function of the wave number of infinitesimal sinusoidal perturbations. Later Trivedi and Kurz [8] extended the linear perturbation theory to the case of large thermal Peclet numbers. Coriell et al. [9] studied the morphological stability of a binary alloy during the initial transient period of directional solidification, in which the interface velocity, concentration and temperature gradients are changing with time. By introducing sinusoidal perturbations of the planar crystal-melt interface they numerically calculated the time evolution of these perturbations. Glicksman [10] reviewed the basic concepts of heat and mass transport surrounding a growing dendrite and also reviewed the dendritic scaling laws and influences of solutal and thermal diffusion on dilute binary alloys. Recently, Schultz et al. [11] studied the incipient instability of growth in polymer blends. They formulated a balance between the breakdown of the solid-liquid interface and stabilization which determines the critical radius of instability of a growing sphere. Their instability analysis includes the Lauritzen and Hoffman interface kinetics and capillarity effects as well.

In this work, the growth of spherulites is modeled first. Situations such as growth in the presence of obstacles and in a temperature gradient are considered with a numerical model. The analytical crystallization models discussed above cannot account for all of these aspects. Such studies have been performed in the past, but the approach in this work is novel and very efficient. A brief outline of the previous work done in modeling associated with polymer processing is presented. Lovinger and Gryte [12] developed a numerical model for the shape of polymer spherulites formed in a temperature gradient. Their model considered the polymer sample to be divided into a series of narrow isothermal regions and, using an analogy to Snell's law [13], correctly predicted the observed fibrillar curvature. Their computer simulation results were consistent with the experimental results. Similarly, Huang and Petermann [14] performed some experiments to model the growth of oriented spherulites

of polybutene-1 in a temperature gradient. When crystallized in a thermal gradient, there is suppression of the nucleation process in the high temperature region and the spherulitic growth is obstructed except towards the higher temperature. They employed a polarizing microscope to study the development of spherulites and demonstrated that a single measurement of the spherulite growth in the temperature gradient was sufficient to calculate many crystallization isotherms. More literature can be found regarding the modeling of spherulites. In this work, modeling of spherulites is carried out using a new concept called the level-set method. Level set methods are numerical techniques which can follow the evolution of interfaces. Rather than follow the interface itself, the level set approach takes a curve representing the interface and builds it into a surface which is called the level set function.

In the second part of this work, a model is derived to account for the diffusion of non-crystallizable species in a blend subjected to a temperature gradient. This is done to determine the possibility of creating in-situ polymer/polymer composites. The simple case of a linear temperature gradient is studied since it is possible to study such systems in the laboratory. Previous research was done on the directional solid-ification of polymers as it is a situation which is encountered in practical problems. Diffusion of non-crystallizable components or segregation of impurities is almost inevitable. It was Keith and Padden [1, 2] who first systematically studied the influence of impurity segregation on the kinetics of spherulitic crystallization. Much later, Ryan and Calvert [15] studied diffusion and annealing in crystallizing polymers followed by which Billingham et al. [16, 17] made a detailed study of the diffusion of stabilizing additives in polypropylene and also of atactic fractions in isotactic polypropylene. The details of all these studies will be mentioned in the subsequent chapters. It is hoped that the model which is developed in this work will allow the modeling of microstructure evolution in more complex systems.

This work constitutes the analytical part of the work funded by Research Excellence Funds. This thesis is divided into six chapters the first of which is this chapter of introduction. The subsequent chapters will focus on the actual work done in this project including some experimental observations related to the directional solidification of the polymer samples.

# Chapter 2

# Crystallization in the Presence of a Temperature Gradient and Solute

#### 2.1 Introduction

Prediction of microstructure formation in polymers is of technological importance as their properties depend on it. A number of studies have therefore been performed to predict the final microstructure of a part and its temperature during cooling. An approach based on the direct numerical simulation of the growth process has been used in the previous chapters. The boundary of each growing spherulite was followed throughout the solidification process and numerical simulations were performed for a small representative volume. In this chapter, the formulations for a theoretical description of the spherulitic growth process in the presence of a temperature gradient, and in the presence of a solute are presented. This material is needed as it is one of the objectives of this study to determine the conditions needed to suppress nucleation ahead of the solid/liquid interface. It is hoped that a cellular morphology will result from the instabilities created by the solute and by suppressing nucleation ahead of the interface.

To begin the analysis, it is important to review the main stages of any non-isothermal process of microstructure formation. These stages are:

- 1] Induction time period: In this time period, the polymer chains reorganize themselves to form nuclei.
- 2] Nucleation: This is the dominant process at the beginning of solidification and leads very rapidly to the establishment of the final spherulite density.
- 3] Growth: This is an important feature of polymer morphology since it could give rise to a variety of morphological units.
- 4] Impurity segregation: Impurities play a major role in determining the crystalline morphology since they are rejected preferentially and their diffusion determines the overall morphology.

Each of these steps will be discussed below and will be supported by relevant case studies. An analysis is then presented to compute the temperature gradient to suppress nucleation ahead of the solid/liquid interface.

## 2.2 Nucleation of Spherulites

Spherulites are the largest microstructural features encountered during the solidification of a quiescent semicrystalline polymer melt. They are polycrystalline aggregates formed from a radiating array of crystalline "ribbons" that branch regularly to create a three-dimensional structure of approximate radial symmetry. According to the mechanism of spherulitic crystallization, after nucleation, lamellae start growing radially to form axialites. These axialites which are the precursors of spherulites, start from stacks of lamellae with a planar geometry to eventually evolve into a full spherical entity. Before delving much into spherulites, an indepth study of the nucleation process will be presented which is responsible for their formation.

Nucleation is generally referred to as the formation of stable nuclei that are able

to grow for a given set of external conditions. Nucleation can be broadly classified into four categories:

- 1] Homogeneous Nucleation: This is referred to as the spontaneous formation of nuclei from the aggregates of polymer chains, when the former exceed some critical size.
- 2] Heterogeneous Nucleation: Nucleation is said to be heterogeneous when nuclei are formed on solid particles already existing in the polymer.
- 3] Thermal Nucleation: A process that occurs throughout the crystallization is referred to as thermal nucleation.
- 4] Athermal Nucleation: This type of nucleation characterizes a solidification process where all the crystals start growing at the same time.

Homogeneous nucleation is connected to thermal nucleation whereas heterogeneous nucleation can be either thermal or athermal. In short, the terms such as homogeneous and heterogeneous characterize the origin of the nuclei while terms such as thermal and athermal characterize the temperature dependence of the nucleation process.

The theoretical treatment of homogeneous nucleation occurring at irregular intervals is based on the ideas developed by Turnbull and Fisher [18], and results in a relation between nucleation rate, N, and temperature T of the following form:

$$N = N_o \exp\left[\frac{-E_D - \Delta G^*}{RT}\right],\tag{2.1}$$

where  $N_o$  is a material constant and is proportional to temperature T,  $E_D$  is the activation energy for transport across the surface of the nucleus,  $\Delta G^*$  is the free-energy of formation of the critical size nucleus and R is the universal gas constant. For a normal three-dimensional nucleus  $\Delta G^*$  is proportional to  $\frac{T_m^2}{\Delta T^2}$ , where  $T_m$  is the melting-point, and  $\Delta T$  is the degree of super-cooling. At small degrees of supercooling

(5 to 20°C) it is thus predicted that the nucleation rate will increase very rapidly with decreasing temperature of crystallization, after an initial period of insensitivity. At much lower temperatures, the  $\frac{E_D}{RT}$  term dominates, so that N passes through a maximum, and subsequently decreases with temperature.

However, homogeneous nucleation almost never occurs in polymers, because of the fact that no polymer melt is pure. It always contains some form of impurity, some nucleating agents or some such solid material. Hence the nuclei tend to form on these existing solid particles thereby characterizing a heterogeneous nucleation. Cormia et al. [19] have shown that heterogeneous nucleation is the dominant mode of nucleation in most of the polymer systems. They used a very ingenious method to support this evidence. Using a fine dispersion of tiny droplets of polyethylene, they found that some particles crystallized at high temperatures of about 125°C, but the majority which were free from heterogeneities or nucleating centers crystallized at much lower temperatures of 90°C. Since the degree of undercooling needed for homogeneous nucleation is far greater than for heterogeneous nucleation, the former is not observed in the practical crystallization of the bulk material

Although heterogeneous nucleation can be either thermal or athermal, the latter is most predominant and will be influencing the nucleation process under study. The modeling of heterogeneous nucleation is a complicated process, since it is necessary to know the distribution of potential nuclei in advance which depends on a large number of factors such as the crystallization temperature, the processing conditions etc. The process is further complicated by the fact that a distinction is made between the apparent and true nucleation rate. While apparent nucleation is found from direct observation of the specimen, the latter is the rate of nucleation of untransformed material accounting for those nuclei which are engulfed by the growing spherulites as well. However, to avoid further complications, it is assumed that the true nucleation

rate is equal to the apparent nucleation rate.

The fact that spherulites in most polymer systems undergo heterogeneous nucleation was further substantiated by Chew et al [20]. They found that the spherulites reappeared in almost identical positions when the sample had been melted and recrystallized. Secondly, both the nucleation rate measurements and the spherulite size distribution diagram confirm that the majority of nuclei form in early stages of transformation which implies that the degree of undercooling is considerably less. During these early stages of transformation, the number of nuclei increases almost linearly with time. It has already been shown by Cormia et al [19] that the nucleation occuring at low degrees of undercooling is essentially due to the presence of heterogeneities and is described as heterogeneous or pseudo-homogeneous nucleation.

Nucleation also can be categorized as isothermal and nonisothermal, depending on the processing conditions. In isothermal nucleation, according to Avrami [4], there is a uniform and fixed density, M, of potential nuclei and they nucleate randomly in time with each nucleus having a probability,  $\nu$ , of developing per unit time. This can be written as

$$\dot{N}(\tau) = \nu M exp(-\nu \tau), \tag{2.2}$$

where  $\dot{N}$  is the rate of nucleation and  $\tau$  is the time function. The nucleation rate is thus an exponentially decreasing function of time. The total number of nuclei as a function of time can thus be written as

$$N(\tau) = M[1 - exp(-\nu\tau)]. \tag{2.3}$$

However, Icenogle [21] found that this equation did not match the experimental data and hence suggested a relation depending on the time of onset of nucleation and time of cessation of nucleation. Many more theories have been developed to describe isothermal nucleation, though all of them require a significant amount of experimental data.

The nucleation process under study is non-isothermal and is most commonly encountered in polymer systems. A model is presented here to describe the nonisothermal nucleation process in which a temperature gradientis imposed on the system. Nucleation can be predicted to a reasonable accuracy with semi-empirical rules, provided all the data for a specific polymer is known, viz. nucleation rate, density, parameters of the nucleation law used, etc. The phenomenon of nucleation depends mainly on the thermal fluctuations which lead to the creation of variously sized spherulites and it also depends on the creation of an interface between the liquid and the solid. Thus it is the thermal fluctuations which lead to the formation of spherulites. The nucleation mechanism is represented by a temperature dependent function given by

$$N = N_r \exp[-\beta_N (T_c - T_r)], \tag{2.4}$$

where  $N_r$  and  $\beta_N$  are fitting parameters.  $N_r$  and  $T_r$  represent the reference nucleation rate and the reference temperature respectively and  $T_c$  is the actual temperature of crystallization. This expression was found to give a satisfactory fit to experimental data describing spherulitic nucleation in polypropylene blends[22]. The result obtained by using published data[22] is shown in Figure 2.1.

The values for  $N_r$  and  $\beta_N$  are  $2 \times 10^{11}/m^3$  and  $0.18/^{\circ}K$  respectively. The reference temperature value was set to  $115^{\circ}C$ . As per the figure, the nucleation rate is seen to be tremendously high for the corresponding range of crystallization temperatures for the polypropylene samples. Such a high rate of nucleation can be attributed to the fact that any commercial polypropylene sample contains one or more nucleating agents which results in the exceptionally high rate of nuclei formation per unit volume of the sample.

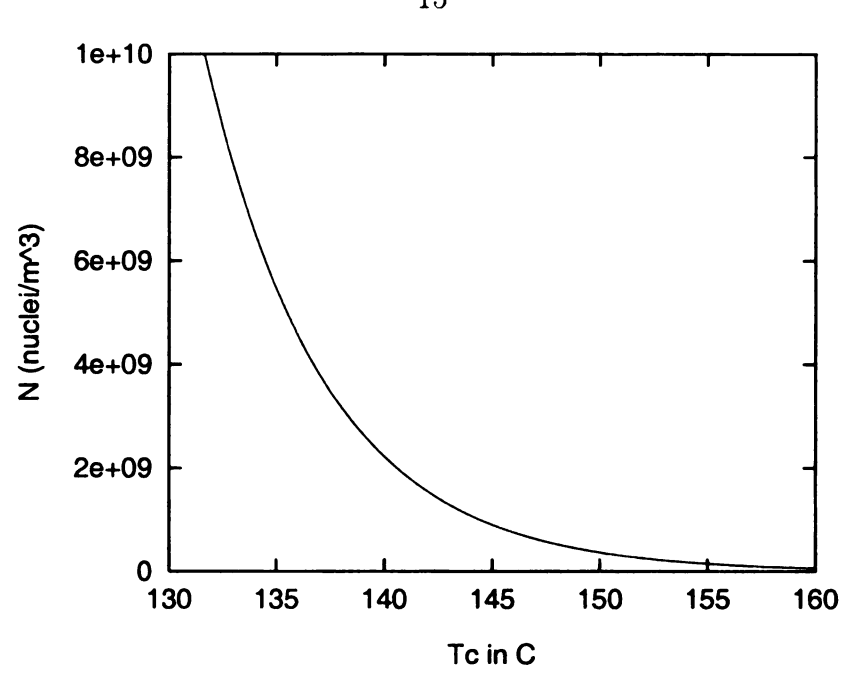


Figure 2.1: Nucleation rate as a function of temperature of crystallization

Since the polypropylene sample under study is devoid of any kind of nucleating agents, the reference rate of nucleation was reduced by two and the nucleation rate was recalculated. The results so obtained are shown in Figure 2.2 which seem to be reasonable

### 2.3 Growth of spherulites

One of the most important features of polymer morphology is the growth process which can give rise to a variety of morphological units. In devising the models of growth mechanisms for polymer crystallization, it is necessary to understand different growth mechanisms which happen to be quite complex in nature in order to establish the most dominant among them for a given set of conditions. During crystallization from the melt, growth may not only involve branching fibrils with defects and amorphous regions, but also it may pass through more than one stage during the course of the process.

The mechanism of spherulitic growth was described as early as 1929 by



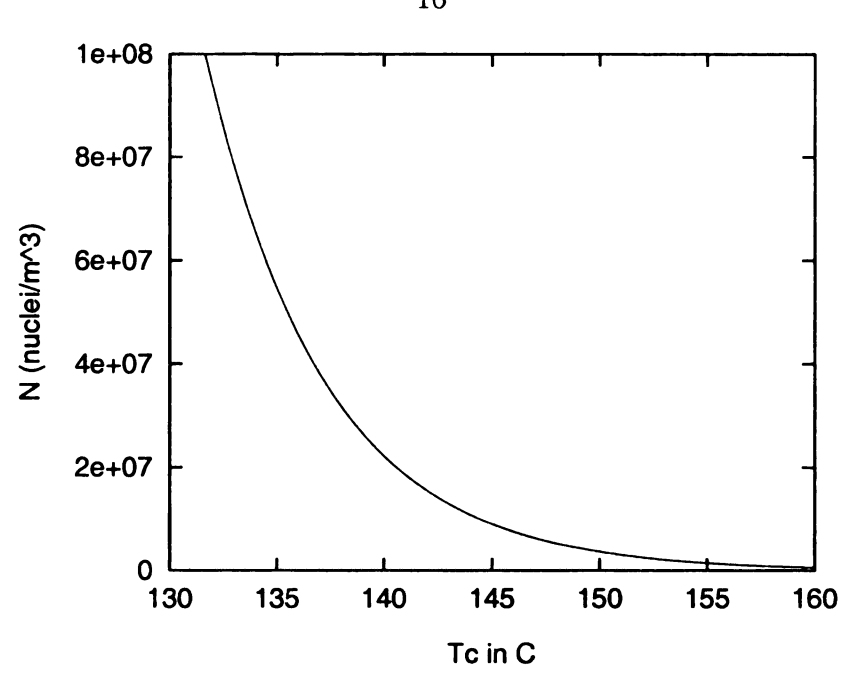


Figure 2.2: New nucleation rate as a function of temperature of crystallization

Bernauer[23]. According to this mechanism, after nucleation, lamellae start growing radially to form axialites, which are precursors of spherulites. The axialites grow to eventually form spherulites by a process in which they start from stacks of lamellae, with a planar geometry, to evolve into a full spherical entity. The work done by Keith and Padden[1] provided the first phenomenological theory of spherulitic growth and experimental observations. They studied the growth of spherulites from polypropylene melts. As discussed before, they postulated that two conditions were required for the formation of spherulites: high viscosity of the medium and the presence of non-crystallizable material. In an isotactic polymer with atactic chains, the atactic portions crystallize less readily than the isotactic components and are rejected from the growing solid. This rejected component is commonly referred to as the "solute". This solute rejected from the crystal creates an excess concentration of impurity which is pushed ahead of the solid/liquid interface. This layer of solute has a bearing on the spherulitic growth. It also has the dual effect of locally depressing the equilibrium crystallization point and reducing the growth rate due to a shortage of crystallizable

material. Thus modeling the growth of spherulites requires that the effects of nucleation, interfacial kinetics, temperature and solute are all accounted for. A brief description of the growth process is given below in the next section.

After the appearance of the nuclei, the growth process is initiated. The growth velocity of spherulites is dominated by interfacial kinetics, rather than by a heat diffusion process [24]. The radial growth velocity in addition to the crystallization temperature,  $T_c$ , is also a function of the composition of the melt in the case of a multi-component system. In case of pure, low molecular weight substances, the growth velocity of spherulites may have a significant magnitude while N, the rate of nucleation, may be very small. This region is referred to as the metastable zone of low subcooling, in which the growth of existing nuclei may proceed without further homogeneous nucleation. The mechanism of growth for spherulitic bodies involves the formation of secondary nuclei. The most important features of any spherulitic growth are the presence of a high viscosity medium and the presence of some dissolved impurity which can be rejected from the growing front. These impurities could be added deliberately or unintentionally present. In polymers though, they are present as branched, atactic or low-molecular weight components, which crystallize less rapidly than the bulk polymer and hence are capable of being rejected during growth. The original theory describing the kinetics of growth was developed by Hoffman and Lauritzen [24]. The growth rate of each branch can be represented in a general manner by the equation

$$\frac{\partial R}{\partial t} = G_o \exp\left[\frac{-U^*}{R(T - T_\infty)}\right] \exp\left[\frac{-K_g}{T\Delta T_f}\right]. \tag{2.5}$$

The first exponential term represents the temperature dependence of the segmental jump rate in the polymer, while the second term is the contribution of the net rate of attachment of new chains to the crystal. R is the spherulite radius and  $G_o$  is a pre-

exponential constant that combines terms not strongly dependent on the material. The growth rate of a polymer crystal therefore results from the rate of deposition of nuclei of a stable size and their subsequent growth, as well as the rate at which untransformed chains are brought to the growing crystal faces.

Similar to the nucleation model, an analytical model is developed for the growth of spherulites. It has been proved by earlier work done that the growth process is controlled by a secondary nucleation step. This can be deduced from the temperature-dependence of the observed growth rates at small degrees of super-cooling. Regardless of the nature of the nucleation process, the growth rate of a polymer spherulite can be described by the equation

$$G = G_r \exp[-\beta_G (T_c - T_r)], \tag{2.6}$$

where  $G_r$  and  $\beta_G$  are fitting parameters.  $G_r$  and  $T_r$  represent the reference growth rate and the reference temperature respectively and  $T_c$  is the temperature of crystallization. This expression was found to give a satisfactory fit to experimental data on the rate of spherulitic growth in polypropylene blends[22]. The result obtained by using some published data[22] is shown in Figure 2.3.

#### 2.4 Directional Solidification

Many attempts have been made to obtain a spherulitic morphology with specific orientation. These techniques involved application of a shear stress on the crystallizing melt and a restriction of the nucleation rate of new spherulites in the melt. Price et al.[25] crystallized PEO from a single nucleation point within a very thin capillary. Sasaguri et al.[26] unidirectionally crystallized a thin film of polybutene-1 in a temperature gradient. Fujiwara et al.[27] and Crissman [28] independently crystallized

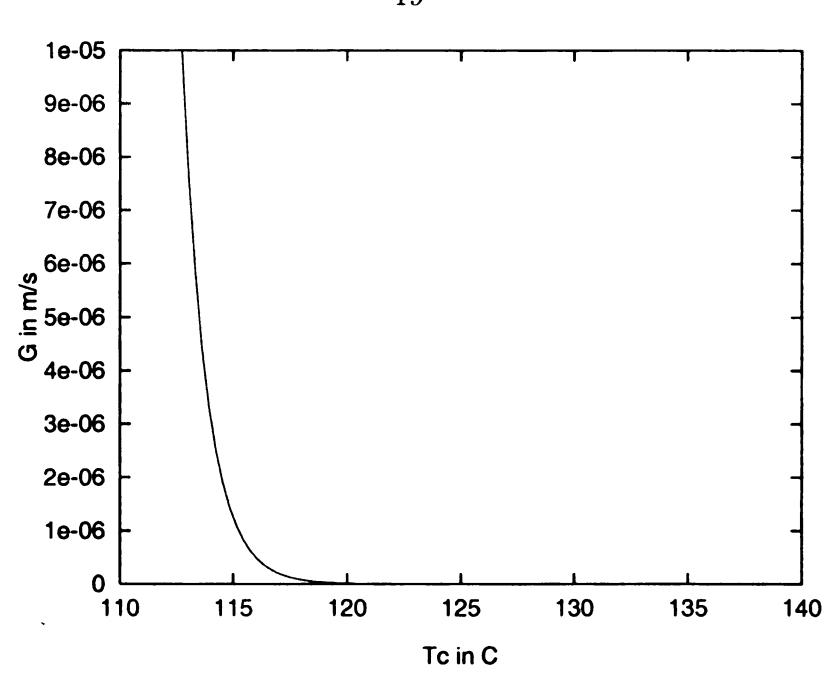


Figure 2.3: Growth rate (m/sec) as a function of temperature of crystallization(°C) for isotactic polypropylene

polypropylene and polyethylene samples using the technique of zone solidification. The process employed in this work is called directional solidification. It has been used for several years in metals and this technique can be adapted to polymer blends in order to manufacture in-situ polymer/polymer composites with enhanced properties compared to the original constituents. It was used by Lovinger et al. [12] to study crystallization of polymers, but no attempt was made to manipulate the microstructure. Directional solidification consists in using a stable linear temperature gradient in such a way, that one part of the sample is above the phase change temperature and the other below it. When the sample is moved through the temperature gradient at a constant velocity the solid/liquid interface remains at the same position and can be observed continuously. This principle is illustrated by a schematic as shown in Figure

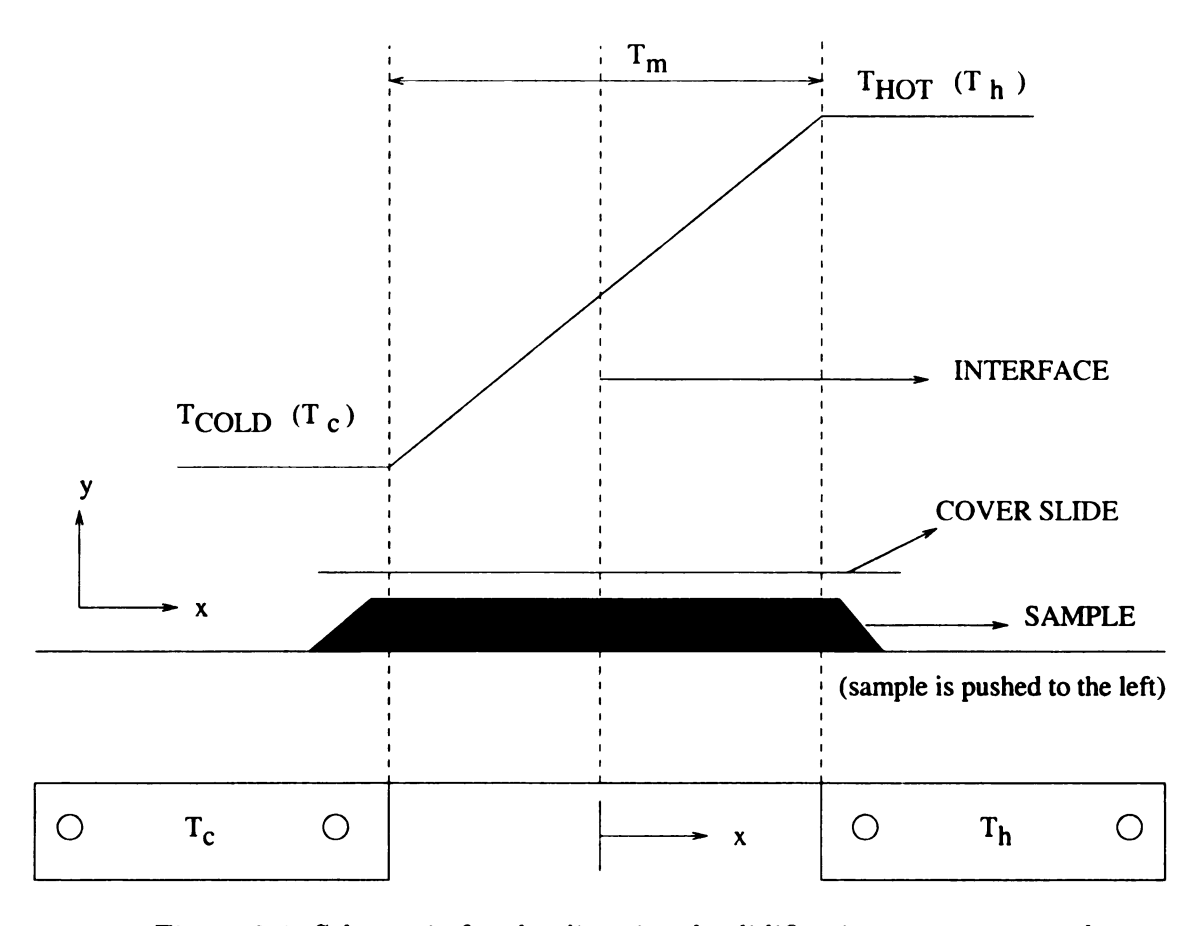


Figure 2.4: Schematic for the directional solidification apparatus used

#### 2.4.1 Problem Formulation and Calculations

The key to obtaining an uninterrupted growth front from a single nucleation point lies in the suppression of the nucleation within the subcooled melt ahead of the growing crystal front. To suppress heterogeneous nucleation, low degrees of undercooling must be used. However, there is a limit to the degree of undercooling that can be employed while at the same time having a reasonable rate of crystallization. In this work, an analysis has been done to determine the case for which single crystal growth can be maintained under conditions where the nucleation rate is not completely suppressed. The analysis is a modified version of the work done by Lovinger et al.[12]. When a molten polymeric material is traversed through a linear temperature profile that brackets its crystallization temperature, crystal growth will be oriented in the direction of the temperature gradient, resulting in long, oblong spherulites. The thermal gradient minimizes nucleation in the high temperature region and this results in oriented spherulites during the crystallization process. A polymer melt sample at temperature,  $T_m$ , and having a cross sectional area, A, is considered for the analysis. If the sample is moving at some velocity, u, through the heated zone, then at a temperature,  $T_c$ , the growth rate, G, is identical with the velocity, u, of the sample. If it is assumed that the temperature gradient,  $T_G$ , is constant over the region of interest, then the temperature at any position, x, below the melting zone is given as:

$$T_c = T_m + T_G x. (2.7)$$

This is the temperature of crystallization where the melt will start crystallizing to form spherulites.

The total number of primary nuclei formed,  $n_T$ , in a sample of cross-sectional

area, A, as it moves from melting point to crystallization point at a velocity, u, is

$$n_T = NV, (2.8)$$

where V is the volume of crystallized polymer and N is the total number of nuclei given by equation (2.4). This equation can also be written as

$$n_T = A \int_0^x N dx, \tag{2.9}$$

which is the same as,

$$n_T = \frac{A}{T_G} \int_{T_m}^{T_c} N dT_c. \tag{2.10}$$

Equation (2.10) is obtained due to a change of variables in equation (2.7). From equation (2.7), it is clear that  $x = \frac{T_c - T_m}{T_G}$ . The variables are changed from x to  $T_c$ . N could be substituted by the expression obtained in equation (2.4). Substituting the value of N and the limits of integration, the equation obtained is

$$n_T = -\frac{N_r A}{T_G} \frac{1}{\beta_N} [\exp(-\beta_N (T_c - T_r)) - \exp(-\beta_N (T_m - T_r))]$$
 (2.11)

The critical condition for a single crystal to be formed that is continuous and devoid of subsequent spherulites is that  $n_T$  be less than unity. Therefore,

$$n_T < 1 \tag{2.12}$$

From equation (2.6),

$$T_c = T_r - \left[\frac{1}{\beta_G} \ln(\frac{G}{G_r})\right]. \tag{2.13}$$

Table 2.1: Values of the parameters from data published in Prog. Polym. Sci

$N_r$	$2 \times 10^9 m^{-3}$	
$eta_G$	$0.916K^{-1}$	
$\beta_N$	$0.18K^{-1}$	
$G_r$	$1.259 \times 10^{-6} \text{ m/s}$	
$T_r$	115°C	

From equations (2.11) and (2.13), equation (2.12) can be written as

$$\frac{-AN_r}{\beta_N} \left[ \left( \frac{G}{G_r} \right)^{\frac{\beta_N}{\beta_G}} - \exp[\beta_N (T_r - T_m)] < T_G.$$
 (2.14)

To compute equation (2.14) values of all the constants and variables that appear in the equation are needed. The values shown in Table 2.1 are known from data published in [22].

In addition, the cross-sectional area of the sample is assumed to be  $1 \times 10^{-6} m^2$ , the melting point as  $200^{\circ}C$  and the growth rate which is same as the velocity of the sample as  $10^{-6}$  m/sec. Substituting all of these values into equation (2.14) the temperature gradient should be approximately  $110^{\circ}C/cm$ , as seen in Figure 3.5. From this equation it is clear that at small cross-sectional areas the volume of the crystallized polymer will be considerably reduced. Hence the solidification carried out in small capillaries or between two narrow glass plates will lead to uniaxial crystallization.

#### 2.4.2 Results and Discussion

It was observed experimentally that the spherical symmetry of the spherulites is distorted in the direction of growth. As the growth rate was reduced, the elongation became more pronounced and the number of nucleation points progressively reduced.

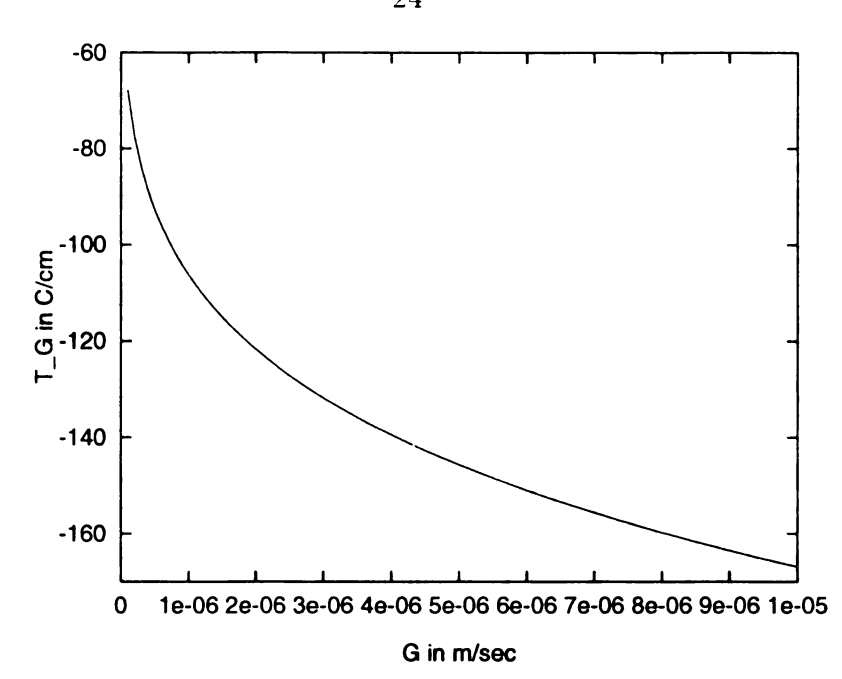


Figure 2.5: Temperature gradient (°C/cm) as a function of velocity of growth front(m/sec)for isotactic polypropylene

At very low velocities, spherulites of unlimited length and oriented in the direction of solidification were grown from the initial nuclei. There exists sporadic nucleation of spherulites within the bulk of the oriented material. This is caused by persistent heterogeneous nuclei. However, only very few of these serve as heterogeneous nuclei for additional nucleation and nucleation is highly suppressed because of the thermal gradient applied. An uniform thermal gradient is assumed across the thickness of the sample. This was numerically verified by calculating the Biot number (hL/k), where h is the convection heat transfer coefficient, L is the thickness of the sample and k is the thermal conductivity of the polymer sample. The Biot number (Bi) provides a measure of the temperature drop in the solid relative to the temperature difference between between the surface and the fluid. For Bi <0.1, it is reasonable to assume a uniform temperature distribution across a soild at any time. It is assumed that h=5  $W/m^2K$ , L = 0.1 mm and k = 0.027 W/m K. For these assumed values, Bi = 0.018. Hence the assumption of a uniform temperature distribution is reasonable, but at the limit of being acceptable. This issue can be addressed in future work.

#### Chapter 3

# Morphological Instability of a Planar Interface during Directional Solidification

#### 3.1 Introduction

During solidification of an alloy, there is interaction of heat and mass transfer processes which can lead to an uneven solidification front. This phenomenon is responsible for the characteristic dendritic structure of alloys. The fundamental explanation for the onset of uneven growth has been provided by the classical Mullins-Sekerka theory of morphological instability[6][7]. This analysis is the key to our understanding of morphological features of solid-liquid interfaces. They developed a rigorous theory of stability by calculating the time dependence of the amplitude of a sinusoidal perturbation of infinitesimal initial amplitude introduced into the shape of the plane. These perturbations are analyzed in terms of infinitesimal sinusoidal Fourier components. They postulated the fact that the interface becomes unstable if any sinusoidal wave grows and is stable if none grow. This theory accurately predicts the

absolute stability of a planar interface at high velocities under constrained growth conditions. However, it suffers from a principal drawback. Their results predicted that a planar interface would be unstable at all velocities in an undercooled melt. This is not true for the case of rapid solidification. Experimental observations have shown the existence of absolute stability of a planar interface in undercooled melts which have been rapidly quenched. Hence some attempts were made to extend their theory to general cases where rapid solidification is encountered. Trivedi et al.[8] reexamined the conventional constitutional supercooling criterion and proposed a more general planar interface stability criterion which is valid for low as well as high growth rate conditions. They derived conditions for absolute stability of pure and alloy undercooled melts and applied their results to dendritic growth from pure undercooled melt.

Among the recent work done on this topic, is the numerical model developed by Coriell et al.[9]. They modeled directional solidification of a binary alloy during the initial transient period in which the interface velocity, concentration, and temperature gradients are changing with time. They introduced sinusoidal perturbations of the planar crystal-melt interface and numerically calculated the time evolution of these perturbations. The results obtained by them were in good agreement with the Mullins and Sekerka analysis, provided instantaneous values of the temperature gradient and solidification velocity are used in the analysis. Schultz et al. [11] examined the results of morphological stability of a polymer crystallizing from a binary melt for large undercoolings. They showed that, for a polymer crystallizing, with its local interface kinetics and rejection of solute, there exists a transition from a compact sphere to a more open one at the point of morphological instability. Jung et al.[29] non-dimensionalised the results obtained by Mullins and Sekerka's stability analysis. By means of a simplified asymptotic analysis of the non-dimensionalised growth rate

equation they derived a single expression for the wavelength of maximum instability.

Their work provided a concise presentation of the stability theory.

## 3.2 Computation of the Solute Concentration Ahead of a Wavy Interface

Under steady-state conditions, the concentrations and solid/liquid interface morphology are independent of time. This implies that the solution to the basic diffusion problem is indeterminate and a whole range of morphologies is permissible from a mathematical point of view. In order to distinguish the solution which is the most likely to correspond to reality, it is necessary to find some additional criterion. Examination of the stability of a slightly perturbed growth form is probably the most reasonable manner in which to treat this situation. The general features of a solidification problem can be described as follows: a solid/liquid interface whose form is defined by a given mathematical function containing one or more variable parameters assumed to be advancing without change into the melt. As it advances, heat and/or solute are evolved at each point of the interface and diffuse into the solid and the melt. The diffusing solute will build up ahead of the interface when k < 1, where k is the solute partition coefficient (ratio of interface concentration in the liquid to that in the solid) and form a boundary layer, while a uniform level of the solute,  $C_o$ , is supposed to exist at a sufficiently large distance from the interface. The boundary layer can be characterised by the ratio of the diffusion coefficient to the growth rate. The diffusion coefficient can be either the thermal diffusion coefficient (in case of the rejection of heat) or the mutual mass diffusion coefficient (in case of the rejection of solute). The thickness of the thermal boundary layer due to the rejection of latent heat is large compared to the scale of microstructures that develop in the polymer blend, which are normally in the micron and sub-micron range. Thus it can be safely assumed that thermal fields have no role to play in the pattern formation, at least for the case of small velocities of growth. The other boundary layer is due to the solute diffusion, in this case the diffusion lengths are small and can scale with the microstructures observed in polymer blends. Hence attention will be restricted here only to the solute diffusion occurring in the liquid.

The basic equation governing any diffusion process is considered [5] and after an extensive mathematical treatment, namely, applying the method of separation of variables and then a suitable set of boundary conditions, a complete solution for the solute distribution is obtained. This equation which represents the solute distribution ahead of a planar solid/liquid interface, advancing under steady-state conditions is written as

$$C = C_0 + (\frac{C_0}{k} - C_0)exp[-\frac{Vz}{D}], \tag{3.1}$$

If the geometry of the problem is such that the interface form corresponds closely to some simple shape, any exact solution which is available for the simple shape can be assumed to be similar to that for the slightly different morphology. The planar solid/liquid interface is then assumed to be changed and the solute distribution calculations for this slightly perturbed solid/liquid interface are made which result in an equation of the form

$$C = C_0 + \left(\frac{C_0}{k} - C_0\right) exp\left[-\frac{Vz}{D}\right] + \left(\frac{kVG_c\epsilon\sin[\omega y]}{Vp - Db}\right) exp\left[-bz\right]. \tag{3.2}$$

Comparing the above two equations, it is seen that the latter has the addition of a perturbation term. In these equations,  $C_o$  represents the initial concentration of the solute, k is the solute partition coefficient, D is the diffusion coefficient in the liquid and V is the velocity of the growth front. In addition, the parameters  $G_c$ , z, b and p

Table 3.1: Assumed values of various parameters

D	$10^{-12}m^2/sec$
k	0.3
V	$10^{-6}m/sec$
$C_o$	0.2
λ	$10^{-6} \text{ m}$
$\epsilon$	$10^{-6} { m m}$

are defined by the following equations:

$$G_c = -V/D(C_o/k - C_o),$$

 $z=\epsilon\sin(\omega y),$  where  $\epsilon$  is the amplitude of perturbation and  $\omega=2\pi/\lambda$  is the wave number,

$$b = \frac{V}{2D} + \sqrt{\frac{V^2}{2D}^2 + \omega^2}$$
 and

$$p=1-k$$
.

Certain values have been assumed for some of the parameters in the above equations. It can be seen that after substituting all these values in the above two equations the solute concentration C is obtained as a function of distance. The plots for the variation of the solute concentration as a function of y for both the planar as well as the slightly perturbed interfaces are shown in Figure 3.1 and 3.2 respectively.

A parameter of major significance in this analysis is the quantity  $\delta = D/G$ , where D is the diffusion coefficient for impurity in the melt, and G is the radial growth rate of a spherulite. The quantity  $\delta$ , whose dimension is that of length determines the lateral dimension of the fibers. From Figure 3.2 it is clear that the lateral dimension of 1e-06 m between the tips of the dendrite correlates well with the actual dendritic spacing seen in the spherulitic growth.

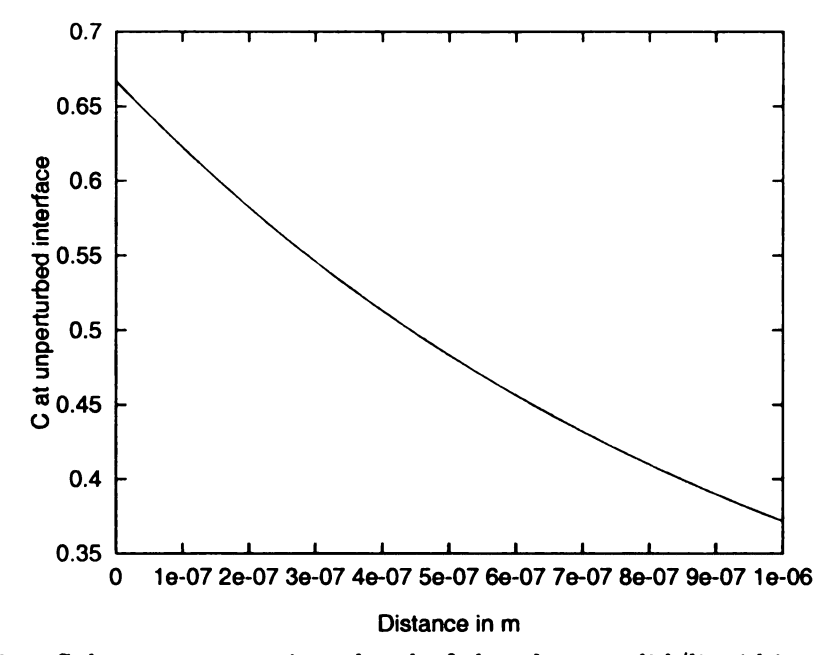


Figure 3.1: Solute concentration ahead of the planar solid/liquid interface

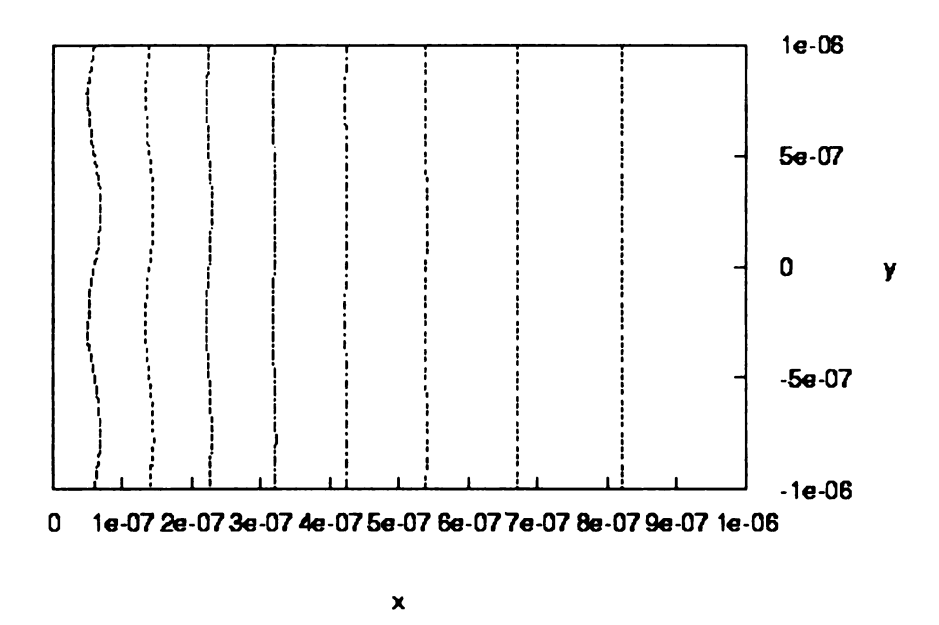


Figure 3.2: Solute concentration ahead of the perturbed solid/liquid interface (x nd y distance is in m)

#### 3.3 Analysis of morphological instability

Classical thermodynamic definitions of stability are inapplicable to the determination of the morphology of a growing interface. Hence it is necessary to use heurestically-based stability criteria. The simplest assumption made is that the morphology which appears is the one which has the maximum growth rate or minimum undercooling. Depending upon the temperature gradient in the liquid melt at the solid/liquid interface there may, or may not, exist a zone of constitutional undercooling. This zone is defined as that volume of the melt ahead of the interface within which the actual temperature is lower than than the local equilibrium solidification temperature. For the existence of such a constitutionally undercooled zone, the temperature gradient at the interface in the liquid should be lower than the gradient of the liquidus temperature in the melt which is simply the product of concentration gradient and the liquidus slope, m. The expression for the concentration gradient is given by equation (3.1). The equation governing this criterion can thus be written as:

$$T_G < -\frac{mV\Delta C_0}{D},\tag{3.3}$$

where  $T_G$  is the temperature gradient at the interface in the liquid, m is the liquidus slope, V is the velocity of the growth front,  $\Delta C_0 = \frac{C_0(1-k)}{k}$  is the concentration difference between the liquid and solid solute contents, where  $C_0$  is the composition of the polymer blend and k is the solute partition or the distribution coefficient. D is the diffusion coefficient in the liquid. This equation is satisfied with the values of parameters assumed in Table 3.1.

This constitutional undercooling criterion provides a useful means for estimating whether a solid/liquid interface will be planar under directional solidification conditions. This is also called the pseudo-thermodynamic criterion for the stability

analysis. The interface will always become unstable so long as this equation is being satisfied. However, this method has several faults. Firstly, it ignores the effect of the surface tension of the interface which will tend to inhibit the formation of perturbations. Secondly, it takes into account only the temperature gradient in the liquid. Thirdly, it does not give any indication of the scale of the perturbations which will develop if an interface becomes unstable. Hence, it is necessary to suppose that the interface has already been slightly disturbed and to see whether the disturbance will grow or disappear. This method is the most famous Mullins-Sekerka criterion for evaluating the interface stability. The mathematical treatment for this theory is very intensive and has been extensively covered in the book by Kurz and Fisher[30]. The mathematical treatment has not been presented here but the final result has been presented for further analysis. The governing equation which is used for the analysis is given as

$$\frac{\dot{\epsilon}}{\epsilon} = \left(\frac{V}{mG_c}\right)(b - \frac{V}{D})(-\omega^2 \Gamma - T_G + mG_c),\tag{3.4}$$

where  $\Gamma$  is the Gibbs-Thomson coefficient,  $mG_c$  is the temperature gradient in the liquid and  $\dot{\epsilon} = \frac{d\epsilon}{dt}$ . The parameter,  $\frac{\dot{\epsilon}}{\epsilon}$ , describes the relative rate of development of the amplitude of a small sinusoidal perturbation. For very small values of  $\omega$ , the value of this parameter is negative due to the curvature damping and the perturbation will tend to disappear. For wave numbers greater than  $\lambda_i$  and above, the sinusoidal shape will become more accentuated. The wavelength having the highest rate of development is likely to become dominant. The reason for the tendency to stability at high  $\lambda$ -values is the difficulty of diffusional mass transfer over large distances. Thus the sign of the parameter determines the stability of the interface. If it is positive for any value of  $\omega$ , then the perturbations with that wave-number will be amplified and they tend to disappear if the value of the parameter is negative. From the calculations it was found that  $\frac{\dot{\epsilon}}{\dot{\epsilon}} > 0$ . This has been graphically shown in Figure 3.3. Hence the

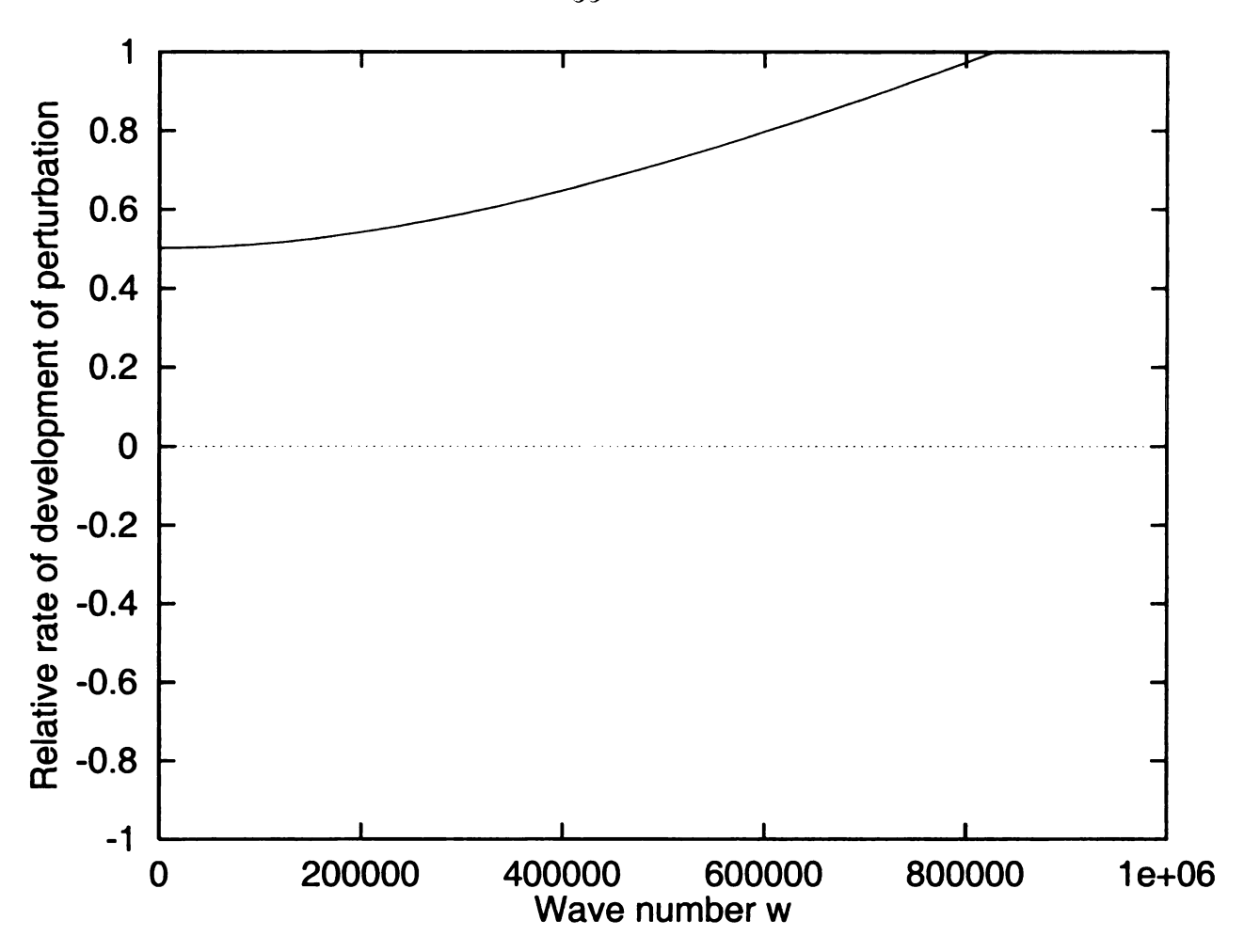


Figure 3.3: Stability criterion for isotactic polypropylene

interface is unstable and the wave number is amplified. The analytical results obtained indicate that the interface concentration at the onset of morphological instability are accurately predicted by the classic Mullins and Sekerka analysis. Once the values of the interface velocity and the temperature gradient at the interface are known, the critical interface concentration can be calculated from the Mullins Sekerka analysis and it is easy to find out if the interface would stabilise or become further unstable.

#### Chapter 4

Using the Eikonal equation to

Model the Phase Change in

Semicrystalline Polymers and their

Composites

#### 4.1 Introduction

Modeling the crystallization of polymers has significant industrial importance since the properties of a product depend on the microstructure developed during processing. For a neat polymer, the main microstructural features observed under the microscope are spherulites. They are aggregates of crystalline plate-like lamellae which grow radially outward from a nucleus.

The spherulitic microstructure defines numerous physical and chemical properties of polymers and its development during processing has been the object of intense research for the past forty years. One of the first quantitative models developed to describe the isothermal evolution of crystallinity in polymers was independently

derived by Avrami [4], Johnson and Mehl [31] and Kolmogorov [32]. The classical analysis of Avrami is often successful in modeling the crystallization process but it also has a number of limitations which have been reported extensively in the past [33]. Among these limitations are variations in the linear growth rate of the spherulites, which may not remain constant at all times. Furthermore, a two-stage crystallization can occur which invalidates the model, and finally the presence of reinforcement such as fibers physically constrains the growth of spherulites and modifies their shape. Analytical models have been developed to predict the effect of fibers on crystallization but they do not account for the "shadow" (merging of fronts behind the obstacle) created by the inclusions in the melt [34] [35]. There was therefore a need to develop a model which could accurately predict the influence of fibers on crystallization and explain many of the unusual features of these systems.

Computer simulation of polymer crystallization is an effective means for studying the crystallization kinetics and morphology development of semicrystalline polymers as they allow flexibility in nucleation and growth models. A significant amount of work has been carried out over the past twenty years and many numerical models have been developed [36][37][38][39][40]. The approach presented below is based on a rapid technique for solving the Eikonal equation[41].

#### 4.2 Factors influencing the spherulitic morphology

The process of spherulitic growth in polymers can give rise to a variety of morphological entities. Extensive experimental and modeling work has been done in the past to study the growth of crystalline forms in many polymer systems. From this work there are three different aspects that affect the morphology: growth in an isothermal field, growth in the presence of fibers and growth of spherulites in the presence of a

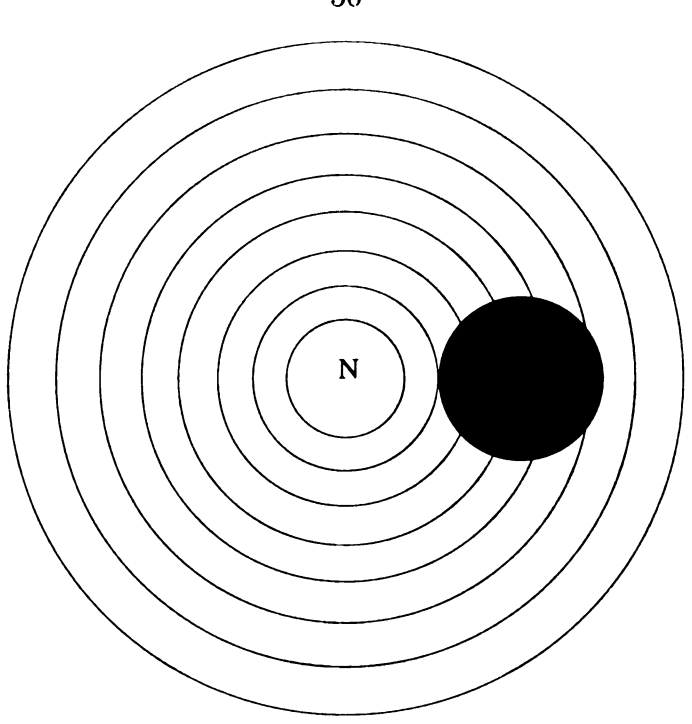


Figure 4.1: Initial concept (now deemed erroneous) used in modeling of a spherulite nucleating at N and growing around a circular obstacle

temperature gradient. These aspects will be discussed briefly below.

Spherulitic growth in isothermal conditions has long been studied. For example, the work done by Keith and Padden [2] provided the first phenomenological theory of spherulitic growth and experimental observations. The spherulitic growth process is initiated after the appearance of the nuclei and the growth velocity of spherulites is often dominated by interfacial kinetics. The growth rate in any isothermal field therefore results from the rate of deposition of secondary nuclei of a stable size and their subsequent growth. A roughly circular entity is formed that may impinge with growing spherulites until solidification is completed.

The growth of spherulites in reinforced polymers has also been an area of study for quite some time. In the isothermal case, each spherulite possesses the same constant growth rate. However, once a spherulite reaches an inclusion in the melt, its growth behavior changes. Initially, the growth of the spherulite as depicted in Figure 4.1 was considered to be the correct description. It was assumed that the spherulite

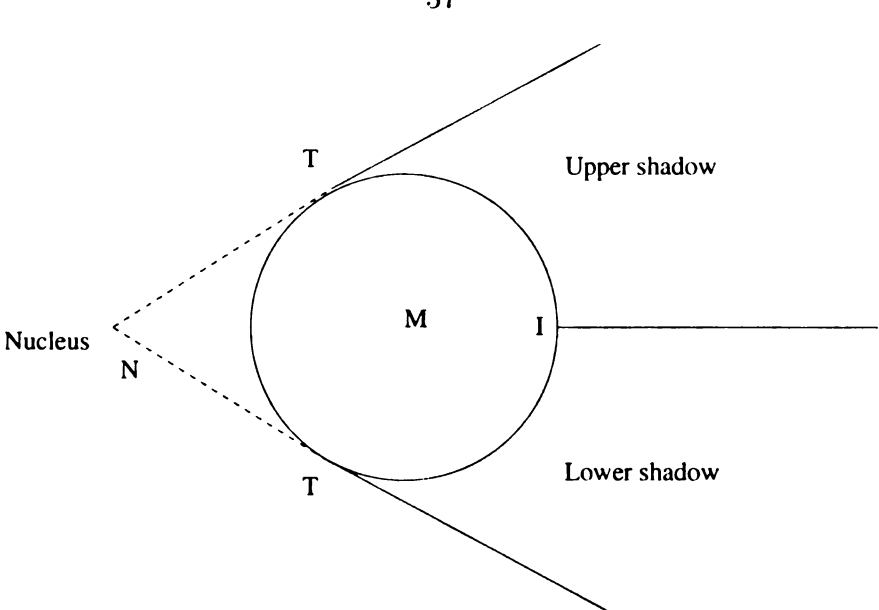


Figure 4.2: A schematic diagram of the shadow behind the circular obstacle with center at M

would grow circularly, whereby the growth through the obstacle was allowed. The growth fronts were always parts of a circle and after the obstacle was totally engulfed, the shape of the growth front was not disturbed just as if no obstacle was present. But the experimental evidence of Schulze et al. [42] as discussed in the previous section indicates that the growth as per Figure 4.1 is incorrect. At all times, the surface of the spherulite stays normal to the surface of the obstacle and it does not remain spherical in shape once an obstacle is encountered. There are certain distinct differences between the growth morphology of spherulites in a neat polymer and those in a polymer composite which have been discussed in detail by Schulze and Biermann [42]. These authors conducted controlled experiments for the case of one spherulite growing around a circular obstacle which is shown schematically in Figure 4.2. It was found that the growth fronts remain perpendicular to the obstacle beginning at the points T in Figure 4.2. The growth is correctly described in the regions outside the "shadow" of Figure 4.2. The "shadow" is limited by two straight lines which are tangential to the border of the obstacle and which pass through the nucleus, N. The

tangent points are denoted by points T. The shape of the spherulite is circular only until it impinges with the obstacle. Once the tangential lamellae come in contact with the obstacle, they grow into the liquid zone behind the obstacle and wrap around it. The growth of spherulites in a thermal gradient was studied by Lovinger et al.[43], among others. They conducted many experiments on samples of polymer systems by directionally-solidifying them in temperature gradients up to  $300^{\circ}$ C/cm and at growth rates down to  $3\mu$ m/min. Highly oriented spherulites are obtained depending upon the temperature gradients, degrees of superheat and pushing velocities employed. Y. Huang [14] also conducted some experiments for polybutene-1 samples. In the low temperature region, the lamellar crystals grow in radial directions. However, once the spherulites are large enough and contact each other, they would grow only into the high temperature region caused by steric hindrance in the direction perpendicular to the thermal gradient. Thus the application of a thermal gradient orients the lamellae parallel to the thermal gradient within the spherulite.

#### 4.3 Previous work done in numerical modeling

Some of the earliest work done in modeling was by Tabar et al.[36] who simulated the two-dimensional spherulitic growth and the effect of impingement on their small-angle light scattering patterns. Galeski and Piorkowska [37] simulated the growth of spherulites for thermal, athermal and combined nucleation mechanisms in both two and three dimensions. These simulations made it possible to examine the influence of the nucleation mechanism on morphological details and verify the results of statistical analyses of spherulite patterns. Some of the recent work in modeling microstructural evolution was done by Billion et al.[38], Krause et al.[40] and Mehl and Rebenfeld [39]. These authors assumed that in a uniform thermal field the spherulites grow radially outward from a spherical nucleus and used cellular discretization to track the growth

of a large population of spherulites and their impingement. Using this approach they could predict the evolution of the microstructure. Billion et al.[38] correctly accounted for the microstructural evolution of a thin film of neat polymer and the impingement of spherulites with the top and bottom surfaces. Similarly Krause et al.[40] modeled the microstructure evolution of a polymer composite assuming that there are no obstacles within the melt and that the entire domain is a neat polymer. The obstacles were accounted for by deleting any volume of the spherulite that lies within an obstacle. This limits their model as it cannot account for the "shadow" behind the obstacle. Mehl and Rebenfeld [39] studied the solidification of polymer composites and modeled the impingement between spherulites and inclusions by stopping growth for all radial directions that intersect the obstacle. This approach is again applicable only when the obstacles are much larger than the spherulites or when the obstacles traverse the entire solidification domain. When these conditions are not satisfied, some errors are introduced when it is compared to real systems. The most recent work done was by Charbon et al. [44] who developed a numerical model for the solidification of semicrystalline thermoplastic polymers. Their model is based on a front-tracking method which accurately predicted the shape of a spherulite but their approach was computer intensive.

Since a number of these methods cannot account for situations where there are small obstacles in the domain or where the growth velocity is a function of both position and time, or the schemes used were computer intensive, it was decided to use a model based on a standard front-tracking method that is efficient and accurate.

#### 4.4 Basis of the simulation

The simulation model presented here for the growth of spherulites is based on solving the two-dimensional Eikonal equation. The Eikonal equation relates the gradient of the travel time to the velocity structure and allows simulation of the propagation of a two-dimensional wavefront for a given growth speed. The eikonal equation is a special case of the Level Set equation which forms the basis of Level Set Methods. They are numerical techniques that offer remarkably powerful tools for understanding, analysing, and computing interface motion in a host of settings. Propagating interfaces occur in a wide variety of settings. As physical entities, they include ocean waves, burning flames, and material boundaries. These interfaces can develop sharp corners, break apart, and merge together. The techniques have a wide range of applications, including problems in fluid mechanics, combustion, manufacturing of computer chips, computer animation, image processing, structure of snowflakes, and the shape of snow bubbles. Rather than following the interface itself, the level set approach takes the original curve and builds it into a surface. This surface is called the Level Set function.

Let t(x,y) be the time at which a curve crosses the point (x,y). The surface t(x,y) then satisfies the Eikonal equation

$$|\nabla t|F = 1, (4.1)$$

where F is the speed of the front.

This equation indicates that the gradient of the time of arrival (t(x,y)) is inversely proportional to the speed of the front. It is a so-called Hamilton-Jacobi equation when the speed function, F, depends only on the position. Figure 4.3 shows the outward propagation of an initial curve and the accompanying motion of the level set function,  $\phi$ . On the left a circle is shown at time t=0 and below it is shown the circle at a later time. In the upper right corner the initial position of the level set function is shown and below we show the same function at a later time. This is referred to as the Eulerian formulation because the underlying coordinate system remains fixed.

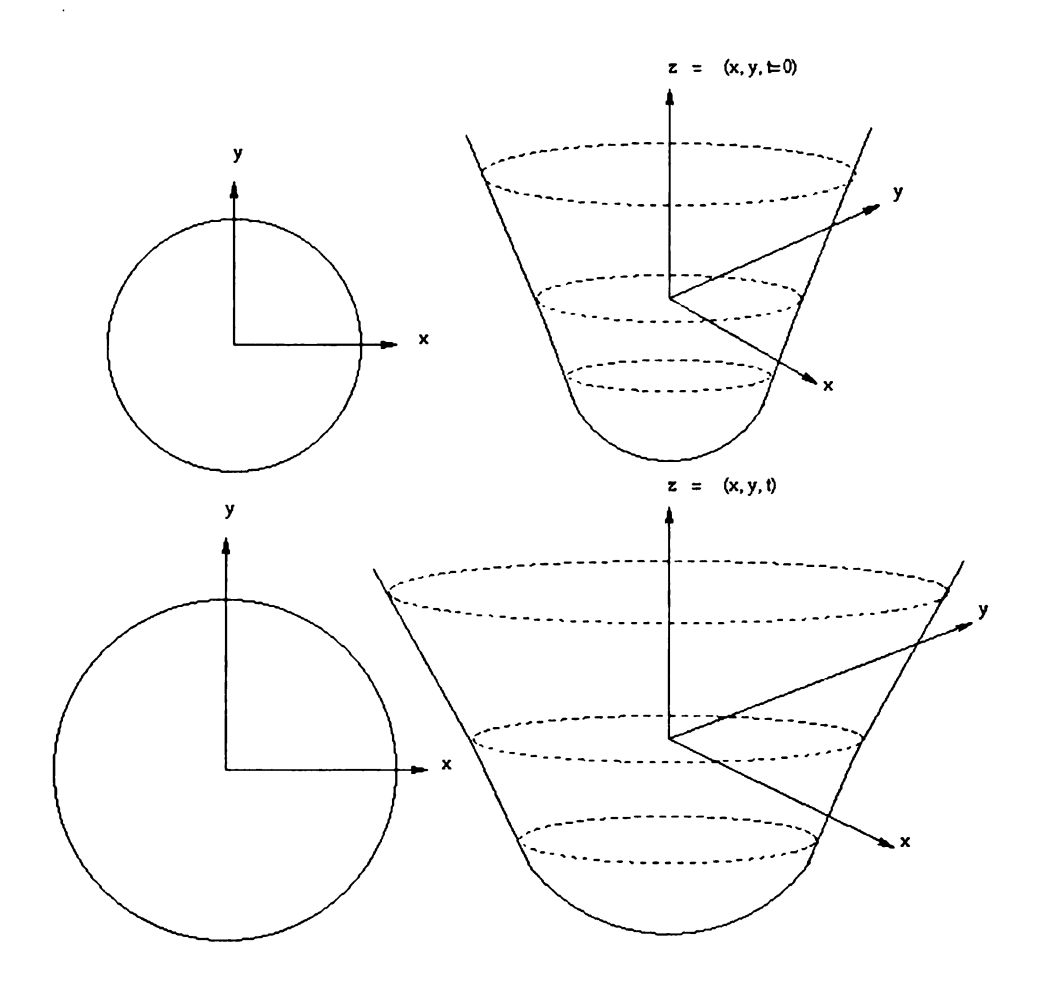


Figure 4.3: Illustration of a propagating circle and the corresponding zero level set

When expressed in Cartesian coordinates, the Eikonal equation takes the form

$$(t_x)^2 + (t_y)^2 = s^2(x, y), (4.2)$$

where s(x,y) is the two-dimensional "slowness" (inverse of velocity or 1/F) and t=t(x,y) is the travel time field. This equation is a non-linear partial differential equation which can be solved using finite difference schemes and a planar wavefront extrapolation.

An optimum numerical method needs to be constructed to solve this partial differential equation. Several methods have been developed to calculate travel times on a regular grid. These methods or schemes are linked to those from hyperbolic conservation laws. From a numerical point of view, the governing partial differential equation can be approximated through the construction of an appropriate numerical flux function, time 't' in our case. The goal in the construction of such flux functions is to make sure that the conservation form of the equation is preserved, to make sure that the entropy condition is satisfied, and to try to produce smooth solutions away from the discontinuities. The majority of these schemes are based on the idea of viscosity solutions, which underly the conservation laws and upwind finite-difference schemes. Therefore it is essential to clearly understand the concept of the viscosity solution of Eikonal equations.

A very important property of viscosity solutions is that these are unique, weak solutions, stable with respect to perturbations in the equation. Since roundoff and discretization errors always perturb a numerical solution, the viscosity solutions are a natural choice of numeric methods. However, the class of weak solutions is too big and the initial data for these problems does not determine weak solutions uniquely. One way to enforce uniqueness of the solution is to add viscosity to the Eikonal equation, where viscosity is described by a dissipative term, which prevents the formation of

gradient discontinuities. Because smooth solutions are uniquely determined by the appropriate initial data, the addition of viscosity fixes the uniqueness problem. The notion of viscosity solutions was developed first for conservation laws, whose weak solutions are made unique by a so-called entropy principle. The entropy solutions of conservation laws are referred to as the viscosity solutions. Conservation laws are commonly solved by upwind finite differencing, using either a backward or forward finite-difference approximation to the derivative operator. Upwind finite-difference methods are stable due to several reasons. Firstly, they add a minimal amount of numerical viscosity to the equations, thereby tending to damp high-frequency error. Secondly, there is no need to specify special numeric boundary conditions or rows of fictitious points for these upstream schemes.

In the present work, two numerical schemes were used to solve equation 4.2. The first one was based on the model developed by Vidale [45] to compute travel times of seismic waves, while the second approach is based on recent work done by Sethian [46].

#### 4.5 Vidale's scheme

The first scheme used in this work was based on the method devised by Vidale [45] which computed travel times of the first arriving seismic waves on a two-dimensional numerical grid by using a finite-difference extrapolation from point to point. The method uses a velocity field that is sampled at discrete points in two-dimensional space, with equal horizontal and vertical spacing. Thus, the nucleus of the spherulite is assumed to be at the grid point A in Figure 4.4. The timing process is initiated by assigning point A the travel time of zero. The four points adjacent to the point A,

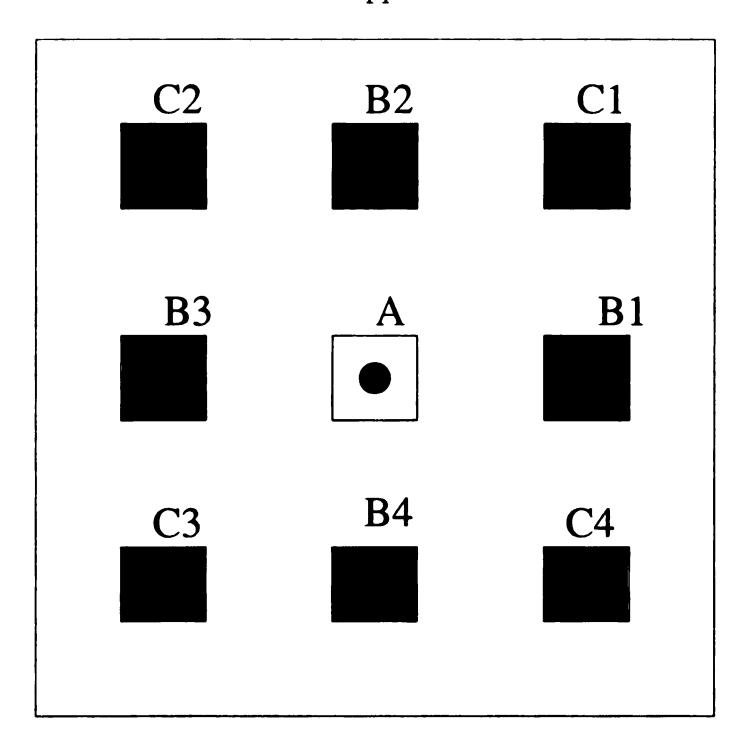


Figure 4.4: A schematic depiction of a source point A (nucleus) and its neighbors in the ring

labeled as  $B_1$  through  $B_4$  are given the travel times

$$t_i = \frac{h}{2}(s_{Bi} + s_A), \tag{4.3}$$

where h is the mesh spacing,  $s_A$  is the slowness at the point A, and  $s_{Bi}$  are the slowness at the grid points  $B_i$ . The formulae that extrapolate the travel times from the three corners of a square to the fourth are derived below. Travel times between the points  $A(t_0)$ ,  $B_1(t_1)$ , and  $B_2(t_2)$  and the origin are sought. The first terms in the equation are an average of two finite difference equations which are written as

$$\frac{\partial t}{\partial x} = \frac{t_0 - t_1}{h},\tag{4.4}$$

and

$$\frac{\partial t}{\partial x} = \frac{t_2 - t_3}{h}. (4.5)$$

An average of these two equations gives

$$\frac{\partial t}{\partial x} = \frac{1}{2h}(t_0 + t_2 - t_1 - t_3). \tag{4.6}$$

Similarly, the second term is an average of the following two equations

$$\frac{\partial t}{\partial y} = \frac{t_0 - t_2}{h},\tag{4.7}$$

and

$$\frac{\partial t}{\partial y} = \frac{t_1 - t_3}{h}. (4.8)$$

The average of these two equations is

$$\frac{\partial t}{\partial y} = \frac{1}{2h}(t_0 + t_1 - t_2 - t_3). \tag{4.9}$$

Substituting equations (4.6) and (4.9) into equation (4.2) gives,

$$t_3 = t_0 + \sqrt{2(hs)^2 - (t_2 - t_1)^2}$$
(4.10)

This equation gives the travel time to point  $C_1$  using the travel times from the source to points A,  $B_1$ , and  $B_2$ . Similarly the arrival times are found for all the other corners. Once all the four corners are found, the times are calculated for the entire ring and the solution can progress to rings of increasing radius. The inductive scheme for adding a ring of travel times to those already calculated is depicted in Figure 4.5. The solution proceeds on the four sides sequentially and is followed by the four corners. The solution could start at any side arbitrarily, however one must take care that the sides are traced sequentially. The critical point in these calculations is that the travel times on any side cannot be calculated in order. The points that are at a

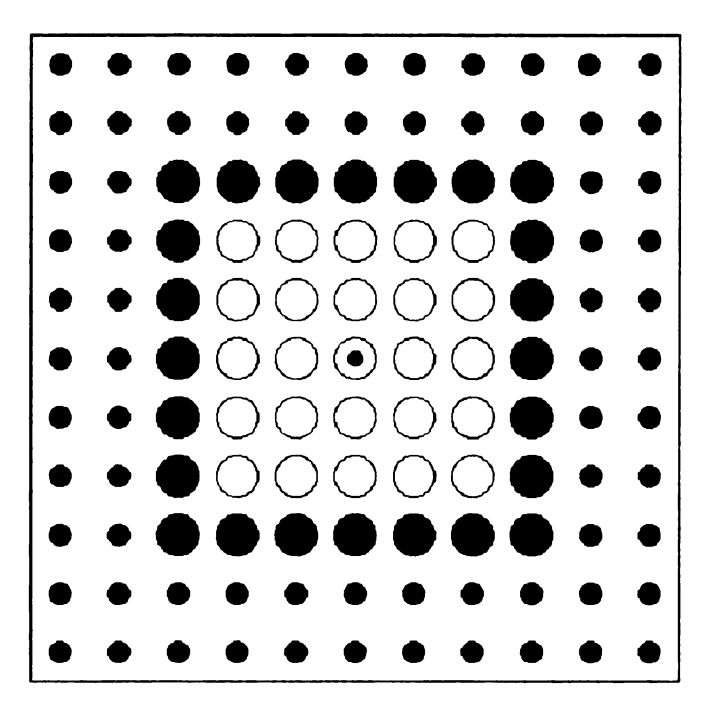


Figure 4.5: A 2-D grid showing the numerical calculation of travel times

relative maximum and relative minimum need to be identified and the calculations can proceed once those points are identified. A relative minimum is assumed if there is a relative minimum in the time for the adjacent point in the adjacent row that has already been solved in the previous ring. The minimum point on any edge is timed using the plane-wave finite difference equation

$$t_3 = t_0 + \sqrt{(hs)^2 - 0.25(t_2 - t_1)^2},$$
 (4.11)

where  $t_3$  is the time to be found,  $t_0$  is the relative minimum time in the inside row, and  $t_1$  and  $t_2$  are the times on either side of the point whose time is  $t_0$ . Once the relative minimum point is found, the solution progresses along the row finding the time for each point until the relative maximum is encountered. Upon completion of the left to right sweep, the row is swept in the reverse direction and the remaining untimed points are solved in order from the relative minima to the relative maxima as shown in Figure 4.6. This method is applied iteratively until the entire two-dimensional grid

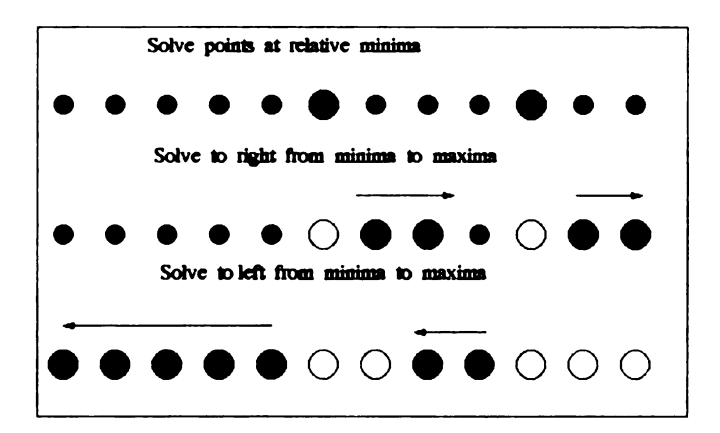


Figure 4.6: An illustration of the sequence of solution of one edge of the ring

The principal drawback of this method is that the points on the computational front must be ordered, with calculations starting at the so-called relative minimum points. This ordering step makes the method computationally expensive. The choice of the computational front is another limitation. Although the solution evolves in time, it is computed by rectangular fronts that expand in space. Thus if the time field to be computed does not have an outward-pointing gradient at each front, i.e. if the time gradient parallels the computational front, the square root in the governing equations (4.10) and (4.11) becomes imaginary and the calculation must stop. This situation occurs when the growth of spherulites occurs in the presence of spatially varying velocity. It fails when the ratio of these two 's' values exceeds a certain limit. The travel times in the ring just outside the obstacle boundary go complex because of the significant changes in the time gradients in and out of the obstacle.

#### 4.6 Sethian's approach

is filled with travel times.

This second approach discussed here is based on the solution of the Eikonal equation as discussed by Sethian [46]. This approach is schematically depicted in the flowchart

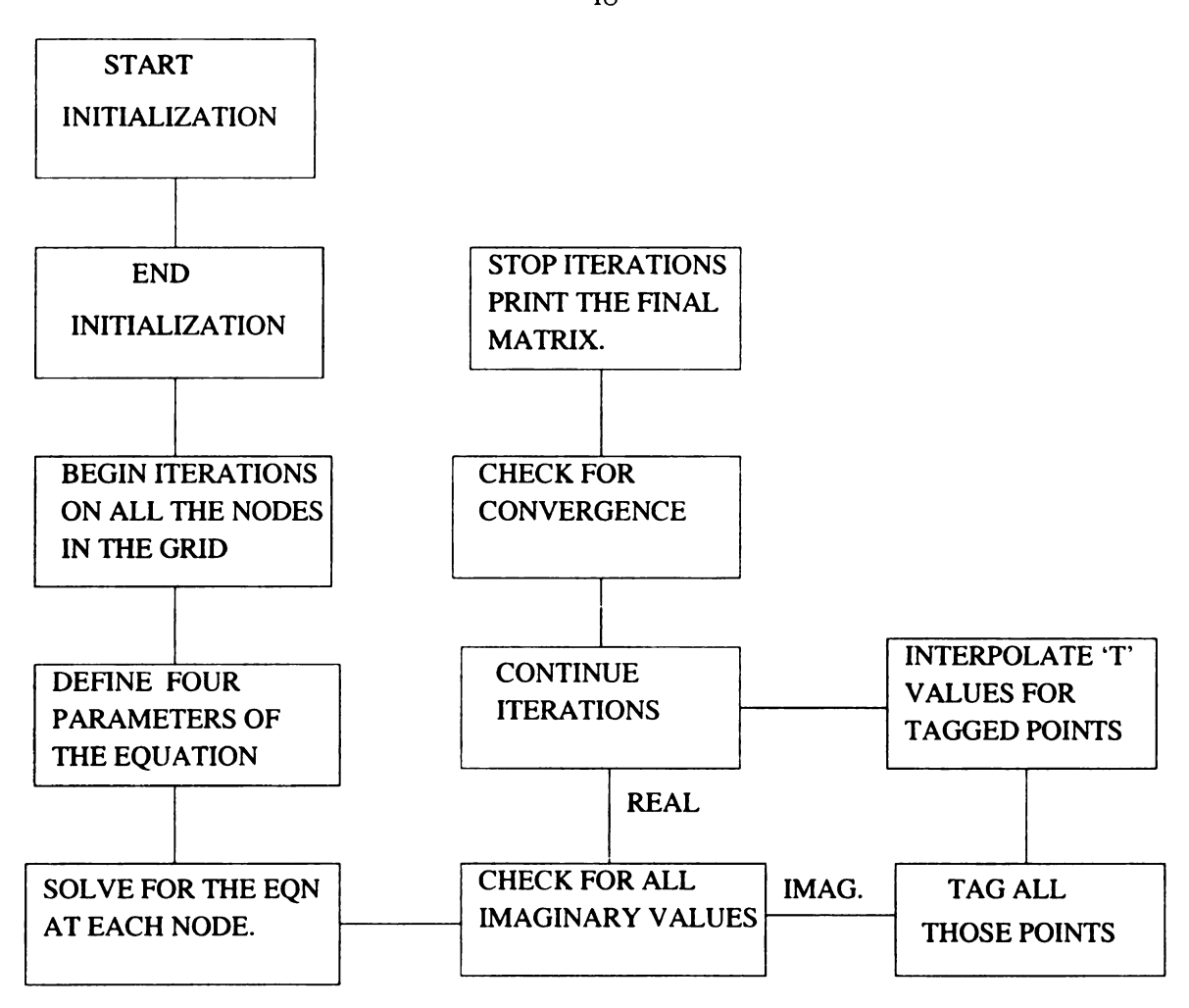


Figure 4.7: Flowchart for Sethian's method

as shown in Figure 4.7. A square grid of size  $N \times N$  was used to model the physical space. In this square box, the solution of the following equation is sought

$$max(D_{ij}^{-x}t,0)^{2} + min(D_{ij}^{+x}t,0)^{2} +$$

$$max(D_{ij}^{-y}t,0)^{2} + min(D_{ij}^{+y}t,0)^{2} = F_{ij}^{-2},$$
(4.12)

where, 
$$D_{ij}^{-x}t = \frac{t_{ij} - t_{i-1,j}}{\Delta x}$$
,  $D_{ij}^{+x}t = \frac{t_{i+1,j} - t_{ij}}{\Delta x}$ ,  $D_{ij}^{-y}t = \frac{t_{ij} - t_{i,j-1}}{\Delta y}$ ,  $D_{ij}^{+y}t = \frac{t_{i,j+1} - t_{i,j}}{\Delta y}$ .

F is the speed function that is positive. F does not depend on the orientation of the front and is simply a function of the applied thermal gradient. This is a quadratic equation which is solved at each grid point. It is solved at each node over the domain until convergence. These iterations are carried out several times through the entire domain and the algorithm consists of:

- (1) Initialization:- The source of the spherulite which is the nucleus is considered to be at the center of the grid. So for a N by N grid, the source point would be at N/2 + 1, which is assigned the time value of zero. All the remaining points in the box are then assigned random values which are increased away from the source point in all directions in equal time steps. So if the origin lies at point (a,b) and the time value at point (a,b) is 't' (zero in this case), points in the positive x-direction would be incremented as  $t + n \times (increment)$ , where "increment" is some fixed value and n is the number of points. Once the time values for all the points on the x-axis are initialized, all other points in the square box are timed similarly. Thus a square grid is obtained filled with all time values which are initial guesses and which represent the growth of a circular entity whose origin lies at the center of the grid.
- (2) Solution:- The smallest time value was selected as a solution of the quadratic equation for every point in the grid. The smallest value was selected to satisfy the so-called entropy condition [46]. This condition ensures that the given surface will sweep through the mesh in a consistent manner and that once the solution is obtained, it is no longer reversible. This procedure of finding the smallest time values is carried out throughout the domain starting at the lowermost left hand corner of the box. At each iteration, the grid is scanned point by point until all the time values are updated. The iterations are carried out several times until a converged solution is obtained. During an iteration, complex solutions are sometimes encountered and these are treated one by one using either an increment over the neighboring value or simply taking an average value of the two neighboring points. If any such points lie on either the x or y-axis, they are incremented over the neighboring value.

#### 4.7 Implementation of the scheme

As discussed earlier in section 4.4, this scheme is linked to hyperbolic conservation laws. The governing equation (4.12) is simply an approximation of a hyperbolic conservation law through the construction of appropriate flux functions. For illustration, the following hyperbolic conservation law is considered

$$u_t + [G(u)]_x = 0. (4.13)$$

From the numerical point of view, the equation can be approximated through the construction of appropriate numerical fluxes, g, such that

$$\frac{u_i^{n+1} - u_i^n}{\Delta t} = -\frac{g(u_i^n, u_{i+1}^n) - g(u_{i-1}^n, u_i^n)}{\Delta x},\tag{4.14}$$

where g(u,u) = G(u). One of the most straightforward approximate numerical fluxes is the Engquist-Osher scheme [47], which is given by

$$g_{EO}(u_1, u_2) = G(u_1) + \int_{u_1}^{u_2} \min(\frac{dG}{du}, 0) \, du. \tag{4.15}$$

For  $G(u) = u^2$ , the compact representation of this flux function is

$$g_{EO}(u_1, u_2) = (max(u_1, 0)^2 + min(u_2, 0)^2).$$
 (4.16)

This flux function is the core technique for approximating the level set equation under consideration. In this problem, for the one-dimensional case,  $u_1 = \frac{t_{ij} - t_{i-1,j}}{\Delta x}$ ,  $u_2 = \frac{t_{i+1,j} - t_{ij}}{\Delta x}$ . This scheme works mainly because it satisfies the condition of consistency and also because each grid point in the domain is updated using the smaller neighboring values. This provides a consistent way of sweeping through the mesh

and constructing the solution surface 't'. The same technique can be extended to the two or three dimensional case. This scheme though very versatile and more generic has certain limitations. It is found that this scheme is extremely sensitive to initial conditions. The validity of the results depend on the way the process of initialization has been done. The simulations were carried out using a variety of initial conditions. Most of the initial conditions tried resulted in a large number of complex numbers and the time values could not be interpolated. It was found that the initialization procedure as discussed in section 4.6 is the most efficient way and the results obtained were very reasonable. Therefore extreme care needs to be taken to assign the initial time values.

#### 4.8 Results and Discussion

The simulations presented below are carried out using Sethian's approach. Though Vidale's scheme gives correct results for single and multiple spherulites, it fails to account for the growth in presence of fibers. The travel times go complex because of changes in the time gradient when the spherulite encounters an obstacle as discussed earlier. Hence the simulations were carried out using Sethian's method as it is versatile and has no limitations. The method is relatively simple and can be used for very large grid sizes. Also, if there are any complex numbers encountered, they can be treated easily.

#### 4.8.1 Spherulitic Growth in a Neat Polymer

Figure 4.8 shows the shape of a spherulite predicted under isothermal conditions using the above scheme. The shape of a spherulite is a circle which has been observed by many experiments [1]. This simulation has been carried out under a uniform melt temperature condition which indicates a constant growth velocity. Thus all the

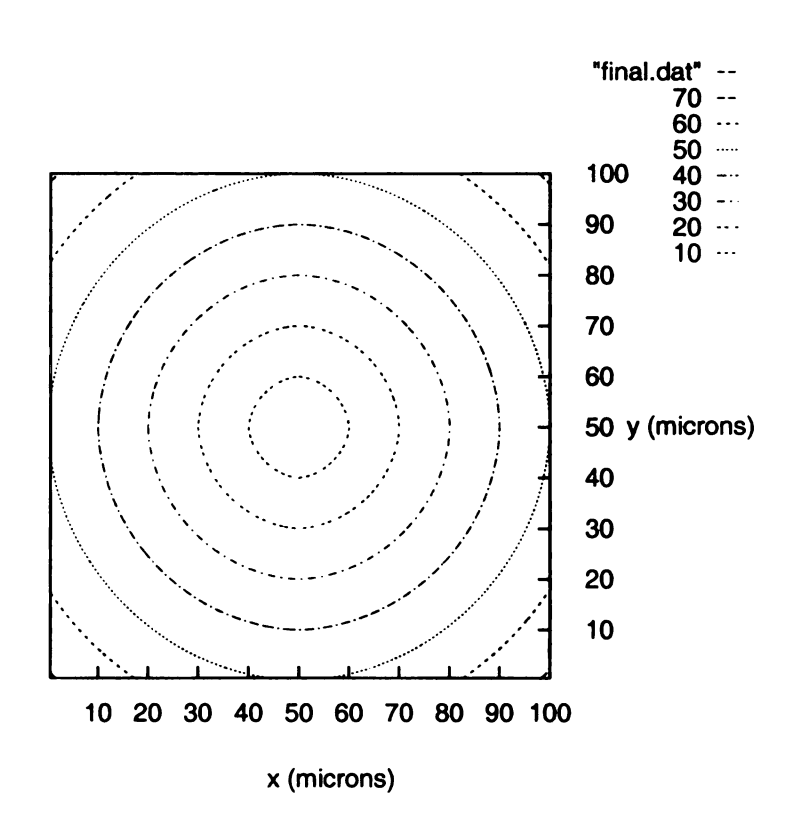


Figure 4.8: Front position of a spherulite at different times while growing in an uniform temperature field (Grid size =  $100 \times 100$  microns and the times are in microns/sec)

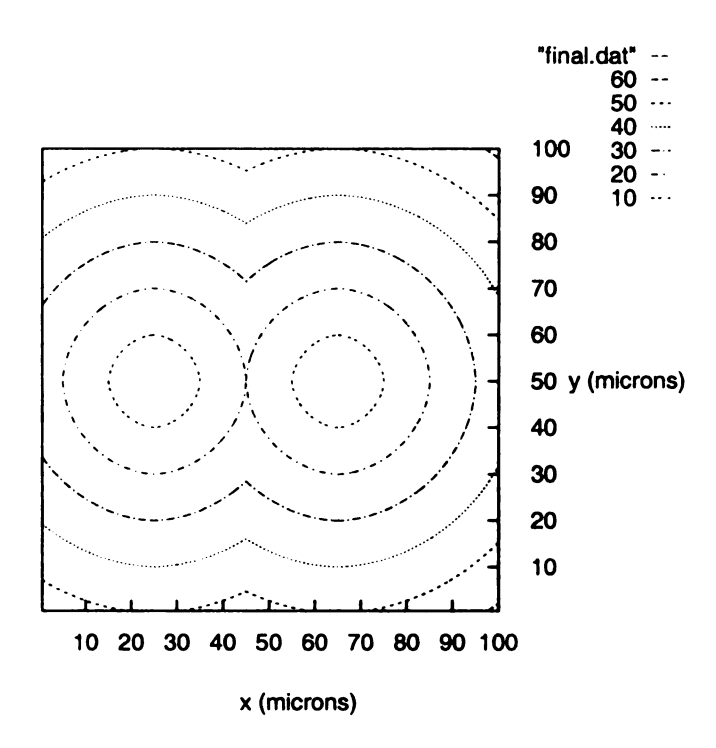


Figure 4.9: Shape of two spherulites at different times illustrating impingement and subsequent growth (Grid size  $= 100 \times 100$  microns and the times are in microns/sec)

spherulites grow with the same velocity. Since the simulations give satisfactory results for single spherulites, we now extend the calculations to two or more spherulites.

Figure 4.9 indicates the growth of two spherulites whose nuclei lie at a certain distance apart in the domain and the solidification progresses at a constant growth velocity. As time progresses, the growth fronts from neighboring spherulites impinge on each other. Figure 4.10 is another such example where the nuclei lie at an off-centered location in the domain.

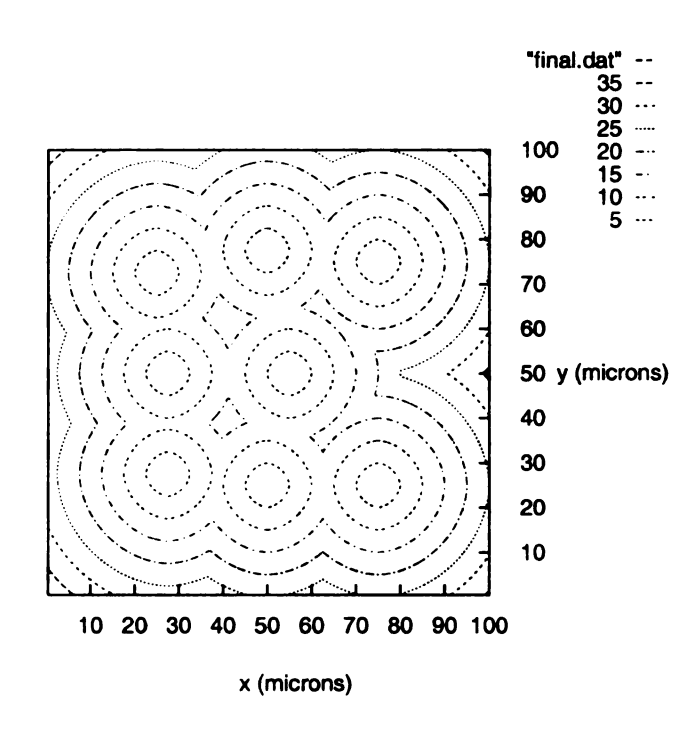


Figure 4.10: Impingement of multiple spherulites with randomly located nuclei shown at different instants (Grid size =  $100 \times 100$  microns and the times are in microns/sec)

#### 4.8.2 Spherulitic Growth in the Presence of Obstacles

The growth of spherulites is also studied in the presence of obstacles which are often present in composites in the form of fibers. The addition of fibers to a given crystallizing system increases the complexity of the system by adding fiber surfaces which can both constrain growth by an impingement mechanism and enhance crystallization by adding nucleation sites. In a first example, a single spherulite growing in the presence of a square inclusion is shown in Figure 4.11. This figure shows that there is an excellent agreement between these results and those obtained by Schulze and Biermann [42] in their experiments. The simulations exactly reproduce the experimental shape of the spherulite for all the time steps. The growth morphology maintains a front normal to the surface of the inclusion as observed experimentally. Figure 4.12 is another case where the obstacles are assumed to be rectangles and randomly distributed within the solidification domain. The modeling is based on the fact that when the spherulite encounters an obstacle, the lamellae that are in contact with the fiber stop growing while the rest of the lamellae continue to grow at the normal speed. Figure 4.12 shows that the simulations give satisfactory results for the presence of multiple obstacles in the domain. For the implementation of the numerical scheme, when an obstacle is encountered, the nodes or points that lie in the region marked as an obstacle, have their local velocity reduced considerably as compared to the growth velocity elsewhere in the solidification domain (typically 1% of the growth velocity). The growth front eventually wraps around the obstacle and a microstructure which maintains a front normal to the surface of the inclusion is obtained.

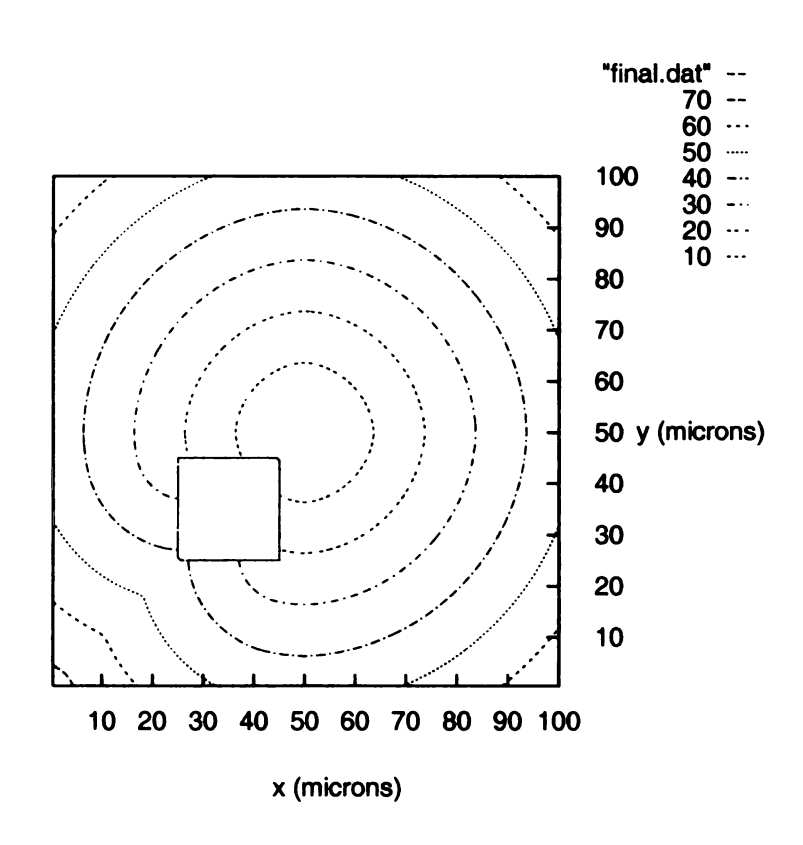


Figure 4.11: Growth of a spherulite in the presence of a rectangular obstacle shown at different times (Grid size =  $100 \times 100$  microns and the times are in microns/sec)

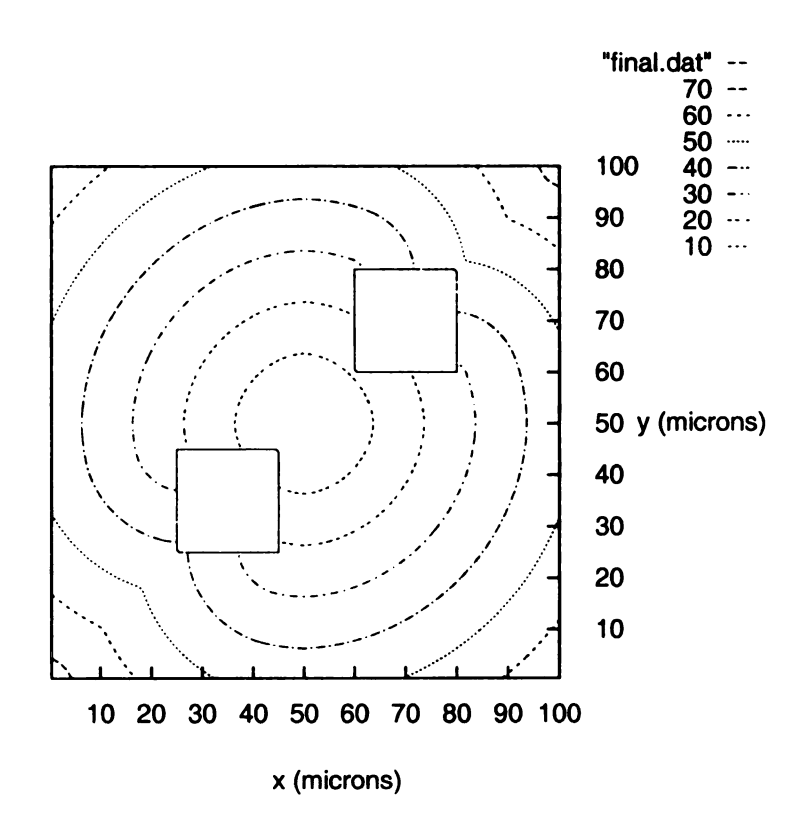


Figure 4.12: Spherulitic growth in presence of multiple obstacles shown at different times (Grid size =  $100 \times 100$  microns and the times are in microns/sec)

### 4.8.3 Spherulitic Growth in the Presence of a Temperature Gradient

Finally, a spherulite that grows in a temperature gradient is considered. This is done to simulate, for example, directional solidification or growth near the wall of a mold where high gradients are present. A linear temperature gradient (of the order of 10<sup>4</sup>°K/m) was applied and the shape of the spherulite obtained from the simulations closely matches the morphological features appearing in the polarization photomicrographs from the work done by Lovinger et al.[43]. The nucleation rate is sufficiently suppressed and the fibrils of the growing spherulite curve towards the direction of motion of the crystallizing front. Figure 4.13 shows this case of the curving of spherulite fibrils from left to right. This shape resembles the teardrop shape obtained in the experiments performed earlier by Lovinger et al.[43], which is the result of the different growth velocities of the solid and liquid phases.

#### 4.9 Conclusions

Two different methods have been discussed in this work which can simulate the growth of spherulites from the melt as a function of the conditions present during the actual solidification process. Both techniques are based on solving the Eikonal equation to track the growth front. Though the first scheme used for modeling is accurate for simulating growth of single or multiple spherulites, it fails to model the growth when there are differences in the local velocities of points due to the appearance of complex numbers during the calculations. The second method proposed by Sethian is more versatile and can predict the time evolution of the shape of a spherulite. The technique is robust and is based on finite difference computation which can be used for a large grid size as well as for growth of multiple spherulites. It can also address the

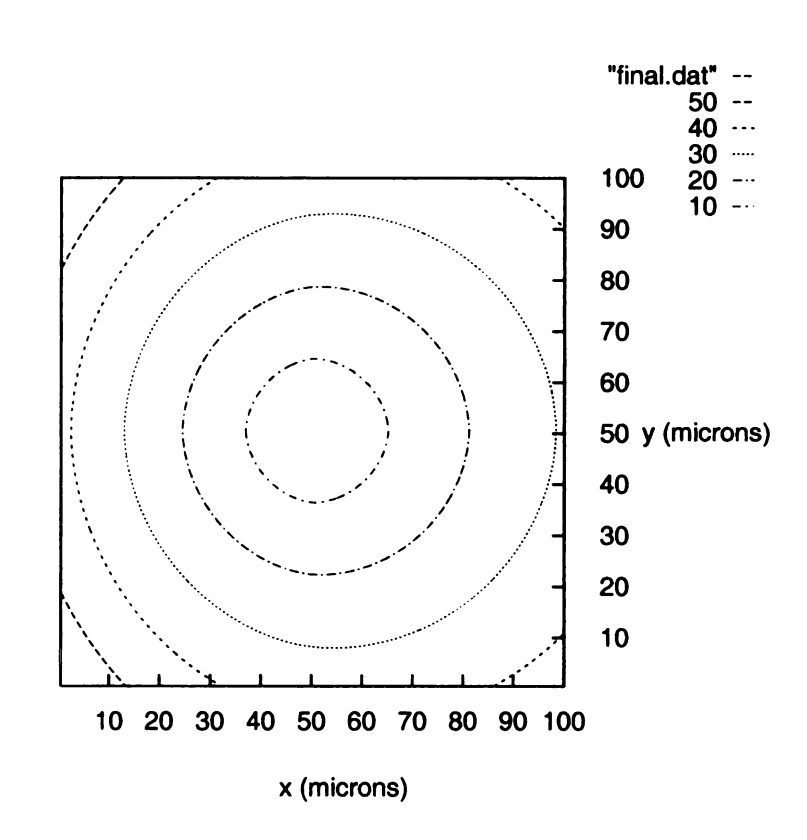


Figure 4.13: Spherulitic growth in the presence of a temperature gradient shown at different times (Grid size =  $100\times100$  microns, times are in microns/sec and dT/dx =  $10^{4\circ} \text{K/m}$ )

problem of the growth of spherulites in the presence of fibers and in the presence of an applied thermal gradient. This was demonstrated with a variety of two-dimensional examples. Both these methods take approximately the same computational times on similar platforms. The simulations were performed on Sun UltraSparc with a CPU speed of 167 MHz and 64 MB Ram. The operating system was SunOS Release 5.6 (UNIX System V Release 4.0). The domain size for the all the results presented was  $100 \times 100$  microns. The approximate time for each simulation performed was 300 seconds.

## Chapter 5

## **Summary and Conclusions**

The solidification of semicrystalline polymers is studied in this work using numerical and analytical models. More specifically, the work presented is directed towards the possibility of using directional solidification to obtain polymer/polymer composites and to model the evolution of the microstructure.

A brief review of the literature pertaining to the types of polymers, and crystallization in semicrystalline polymers was first presented. A numerical scheme to describe the evolution of spherulites under various conditions was then presented Two different methods were employed to simulate the growth of spherulites, Vidale's scheme and Sethian's approach. Both these techniques were based on solving the Eikonal equation. The method proposed by Sethian is more versatile and can predict the time evolution of single and multiple spherulites, growth of spherulites in the presence of fibers and also in the presence of an applied thermal gradient. Several simulations were carried out to demonstrate these methods. The cases of isothermal crystallization, crystallization in a temperature gradient, and crystallization in the presence of obstacles are considered and various examples are solved for two-dimensional processes. Crystallization of a homogeneous polymer blend composed of a non-crystallizable polymer and a crystallizable polymer was then considered. An-

alytical work was done directed towards studying the possibility of forming in-situ polymer/polymer composites using directional solidification. The vital stages of the non-isothermal processes of microstructure formation such as nucleation and growth were discussed. The thermal conditions that favor steady growth and which suppress nucleation ahead of the growing interface were identified. The stability issues of the growing interface were then addressed. It was shown that for the given problem under consideration, the interface always became unstable, which gave rise to crystalline fingers in the direction of the thermal gradient. The work presented here is hoped to serve as the basis for future engineering designs of materials and processes related to this new type of composite. Shrinkage and drawability of these new materials are expected to be very good, with improved mechanical properties compared to the pure amorphous polymer. It is hoped that this work will enhance our understanding of the crystallization process in polymers. Also, the numerical model presented is a versatile model describing the shape of polymer spherulites formed in a temperature gradient. The computational times are very short as compared to other models developed.

## Chapter 6

## Suggestions for Future Work

In this work, an efficient two-dimensional numerical model has been developed that satisfactorily predicts the microstructure and crystallization kinetics of polymer composites. However it would be more realistic to develop a model that can perform three-dimensional simulations. The present model considers instantaneous nucleation in an isothermal field. Future work could involve the study of the influence of the mode of nucleation and the functionality of the spherulitic growth rate. The numerical model presented here simulates the growth of spherulites in the presence of obstacles, but it does not consider the types and size of fibers. A close examination could be made of the effect of fiber size and shape on the crystallization process in reinforced systems for both two and three dimensional cases. Once the three-dimensional model is accurately developed it can be coupled with a finite element code developed. A model based on an enthalpy formulation of the energy equation can simulate the solidification process occuring in complex three-dimensional parts when combined with these simulations. It will thus be possible to compare the observed morphology of a complex part with the computed results.

It was also found in the course of performing the simulations that the initial conditions have some influence on the rate of convergence of the numerical scheme.

A combination of both Vidale's and Sethian's schemes might provide a methodology that will improve the convergence of the algorithm.



## Appendix A

# C code based on Sethian's approach

```
% This is the main simulation program based on Sethian's approach%
#include<stdio.h>
#include<math.h>
double T[300][300], TNEW[300][300];
double F[300][300];
double slowF[300][300];
int N = 200;
double dX, dY;
float initVal = -0.05;
float finVal;
float orgVal = 0.0;
float tol =0.0000010;
float sum;
float incr;
```

```
int obsLen, obsBrt, obsOrgX, obsOrgY;
struct _obj
{
  int obsLen;
  int obsBrt;
  int obsOrgX;
  int obsOrgY;
}
object[100];
double min(double x, double y)
{
  if(x<y) return x;</pre>
  else return y;
}
double max(double x, double y)
{
  if(x>y) return x;
  else return y;
}
main()
{
  int i, j, a, b, k, counter;
  int flag1, flag2, flag3, flag4;
  float fact1, fact2, fact3, fact4;
  double A, B, C;
  /* double xdim=100; */
  double rootVal;
  double p,q;
```

```
int iter=0;
  int n_objects;
  int done=0;
  int centX[5], centY[5], cents, NO_CENTS;
   incr = 10.0;
    dX = dY = 1.0/N;
    for(i=0; i<N+2; i++)
    for(j=0; j<N+2; j++)
      {
F[i][j] = .01;
slowF[i][j] = 0.000001;/*1/F[i][j];*/
      }
  printf("Give no. of objects\n");
  scanf("%d",&n_objects);
 for(i=0; i<n_objects; i++)</pre>
    {
      printf("Give obs. length\n");
      scanf("%d",&object[i].obsLen);
      printf("Give obs. breadth\n");
      scanf("%d",&object[i].obsBrt);
      printf("Give obs. xorigin\n");
      scanf("%d",&object[i].obsOrgX);
     printf("Give obs. yorigin\n");
      scanf("%d",&object[i].obsOrgY);
```

```
}
printf("Data inputed:\n");
for(i=0; i<n_objects; i++)</pre>
   {
     printf("%d ",object[i].obsLen);
     printf("%d ",object[i].obsBrt);
     printf("%d ",object[i].obsOrg%);
     printf("%d\n",object[i].obsOrgY);
   }
printf("print the centers, print -1 -1 to stop : \n");
NO_CENTS=0;
 for(i=0;i<5;i++)
   {
     scanf("%d %d", &centX[i], &centY[i]);
     if(centX[i]==-1) break;
     NO_CENTS++;
   }
for(cents=0;cents<NO_CENTS;cents++)</pre>
   {
    a = centX[cents];
    b = centY[cents];
    T[a][b] = orgVal;
    for(k=b+1; k<=N+1; k++)
```

```
{
 T[a][k] = T[a][k-1]+incr;
}
      for(k=b-1; k>=0; k--)
{
 T[a][k] = T[a][k+1] + incr;
}
      for(i=b; i<=N+1; i++)
{
 for(j=a+1; j<=N+1; j++)
   {
      T[j][i] = T[j-1][i] + incr;
   }
  for(j=a-1; j>=0; j--)
   {
     T[j][i] = T[j+1][i] + incr;
   }
}
      for(i=b; i>=0; i--)
{
 for(j=a+1; j<=N+1; j++)
   {
      T[j][i] = T[j-1][i] + incr;
   }
  for(j=a-1; j>=0; j--)
    {
```

```
T[j][i] = T[j+1][i] + incr;
    }
}
    }
  while(1)
    {
      for(j=1; j<N+1; j++)
{
  for(i=1; i<N+1; i++)
    {
if( (i==a) && (j==b) ) continue;
      fact1 = (T[i][j] - T[i-1][j])/dX;
      fact2 = (T[i+1][j] - T[i][j])/dX;
      fact3 = (T[i][j] - T[i][j-1])/dY;
      fact4 = (T[i][j+1] - T[i][j])/dY;
      flag1=flag2=flag3=flag4=1;
      if(fact1<=0.0) {fact1 = 0.0;flag1=0;}
      if(fact2>=0.0) {fact2 = 0.0;flag2=0;}
      if(fact3<=0.0) {fact3 = 0.0;flag3=0;}</pre>
      if(fact4>=0.0) {fact4 = 0.0;flag4=0;}
      A = (flag1+flag2)*dY*dY + (flag3+flag4)*dX*dX;
     B = -2*(dY*dY*(T[i-1][j]*flag1+T[i+1][j]*flag2) +
```

```
dX*dX*(T[i][j-1]*flag3+T[i][j+1]*flag4));
      /* if( (i>obs0rg%) && (j>obs0rg%) ) */
      for(counter=0;counter<n_objects;counter++) {</pre>
obsLen = object[counter].obsLen;
obsBrt = object[counter].obsBrt;
obsOrgX = object[counter].obsOrgX;
obsOrgY = object[counter].obsOrgY;
if( (i>obsOrgX) && (i<obsOrgX+obsLen) && (j>obsOrgY)
&& (j<obsOrgY+obsBrt) ) {
  done=1;
  break;
}
      }
      if(done)
C = dY*dY*(T[i-1][j]*T[i-1][j]*flag1+T[i+1][j]*T[i+1][j]*flag2)
    + dX*dX*(T[i][j-1]*T[i][j-1]*flag3+T[i][j+1]*T[i][j+1]*flag4)
     - dX*dX*dY*dY/(slowF[i][j]*slowF[i][j]);
      else
C = dY*dY*(T[i-1][j]*T[i-1][j]*flag1+T[i+1][j]*T[i+1][j]*flag2)
    + dX*dX*(T[i][j-1]*T[i][j-1]*flag3+T[i][j+1]*T[i][j+1]*flag4)
            - dX*dX*dY*dY/(F[i][j]*F[i][j]);
      done=0;
      if ( (A == 0.0) \mid | ((B*B-4.0*A*C) < 0.0) )
TNEW[i][j] = -3.00;
```

```
else
TNEW[i][j] = (-B+sqrt(B*B-4.0*A*C))/(2.0*A);
    }
}
      for(i=1; i<N+1; i++)
{
 for(j=1; j<N+1; j++)
    {
      if(TNEW[i][j]!=-3.00) continue;
      /*find quadrant*/
      if((i>a) && (j>b)) /*1st*/
{
 p = max(TNEW[i-1][j], TNEW[i][j-1]);
 q = min(TNEW[i][j+1], TNEW[i+1][j]);
  if(p==-3.0)
   printf("p==-3.0\n");
 else if(q==-3.0)
    TNEW[i][j] = p + incr;
 else if( (i==N) || (j==N) )
    TNEW[i][j] = p+incr;
 /*else if(p>=q)
    TNEW[i][j] = p+incr;*/
  else
```

```
TNEW[i][j] = (p+q)/2.0;
}
      else if( (i<a) && (j>b) ) /*2nd*/
{
  p = max(TNEW[i+1][j], TNEW[i][j-1]);
  q = min(TNEW[i][j+1], TNEW[i-1][j]);
  if(p==-3.0)
    printf("p==-3.0\n");
  else if((TNEW[i+1][j]==-3.0) || (TNEW[i][j+1]==-3.0))
    TNEW[i][j] = (TNEW[i][j-1] + TNEW[i-1][j])/2.0;
  else if( (i==1) || (j==N) )
    TNEW[i][j] = p+incr;
  /*else if(p>q)
    TNEW[i][j] = p+incr;*/
  else
    TNEW[i][j] = (p+q)/2.0;
}
      else if( (i<a) && (j<b) ) /*3rd*/
{
 p = max(TNEW[i+1][j], TNEW[i][j+1]);
  q = min(TNEW[i-1][j], TNEW[i][j-1]);
  if(q==-3.0)
   printf("p==-3.0\n");
  else if (p==-3.0)
```

```
TNEW[i][j] = q + incr;
  else if((TNEW[i+1][j]==-3.0) || (TNEW[i][j+1]==-3.0))
    TNEW[i][j] = q + incr;
  else if(i==1)
TNEW[i][j]=TNEW[i-1][j]-incr;
else if (j==1)
TNEW[i][j]=TNEW[i][j-1]+incr;
  else if(p>q)
    TNEW[i][j] = p+incr;
  else
    TNEW[i][j] = (p+q)/2.0;
}
      else if( (i>a) && (j<b) ) /*4th*/
{
  p = max(TNEW[i][j+1], TNEW[i-1][j]);
  q = min(TNEW[i][j-1], TNEW[i+1][j]);
  if(p==-3.0)
    printf("p==-3.0\n");
  else if (q==-3.0)
    TNEW[i][j] = (TNEW[i][j-1] + TNEW[i-1][j])/2.0;
  else if( (i==N) || (j==N) )
    TNEW[i][j] = p+incr;
  else if(p>q)
    TNEW[i][j] = p+incr;
  else
    TNEW[i][j] = (p+q)/2.0;
```

```
}
      else if(j==b) /*x axis*/
{
  if(i>a) /*+ve*/
    TNEW[i][j] = TNEW[i-1][j]+incr;
  else
    TNEW[i][j] = TNEW[i+1][j]+incr;
}
      else if(i==a) /*y axis*/
{
  if(j>b) /*+ve*/
    TNEW[i][j] = TNEW[i][j-1]+incr;
  else
    TNEW[i][j] = TNEW[i][j+1]+incr;
}
      else
printf("OUTTA MY HANDS\n");
      /* west */
      if(i==1)
{
 TNEW[i-1][j] = TNEW[i+1][j];
}
```

```
/* east */
      if(i==N)
{
  TNEW[i+1][j] = TNEW[i-1][j];
}
      /* n*/
      if(j==N)
{
  TNEW[i][j+1] = TNEW[i][j-1];
}
      TNEW[a][b]=0.0;
    }
}
      /*compare T & TNEW*/
      sum=0.0;
      for(i=1; i<N+1; i++)
for(j=1; j<N+1; j++)
  sum += (T[i][j]-TNEW[i][j])*(T[i][j]-TNEW[i][j]);
      /*if NOT OK, copy T to TNEW */
      printf("DIF = %f\n", sum);
      if(sum <= tol) break;</pre>
      for(i=1; i<N+1; i++)</pre>
```

```
for(j=1; j<N+1; j++)
  T[i][j] = TNEW[i][j];
      iter++;
      if(iter>600) break;
    } /*end of while*/
  finale:
  printf("The final Matrix\n");
  for(i=1; i<N+1; i++)
    {
      for(j=1; j<N+1; j++)
printf("%2.2f ", TNEW[i][j]);
      printf("\n");
    }
  printf("# of iters=%d\n", iter);
}
```

## Appendix B

## Matlab program for simulations based on Vidale's scheme

### B.1 mex.m

```
end
    end
    end
    end
ring(xpo,ypo)=t0+sqrt((2*(hs^2))-((t2-t1)^2));
prevrin=t0+sqrt((2*(hs^2))-((t2-t1)^2));
valuecorn=t0+sqrt((2*(hs^2))-((t2-t1)^2));
if(gr>1)
for chek=1:10
        if(sid==1)
 if(least(4*(gr-2)+1,chek)==xpo)
            t0=ring(xpo,ypo-1);
          t1=ring(xpo+1,ypo-1);
          t2=ring(xpo-1,ypo-1);
          ring(xpo,ypo)=t0+sqrt(((hs^2))-.25*((t2-t1)^2));
          valuecorn=t0+sqrt(((hs^2))-.25*((t2-t1)^2));
          side1=1;
          xpo=xpo;
          ypo=ypo;
         %pause
        end
     end
      if(sid==2)
        if(least(4*(gr-2)+2,chek)==ypo)
   t0=ring(xpo+1,ypo);
         t1=ring(xpo+1,ypo+1);
         t2=ring(xpo+1,ypo-1);
         ring(xpo,ypo)=t0+sqrt(((hs^2))-.25*((t2-t1)^2));
```

```
valuecorn=t0+sqrt(((hs^2))-.25*((t2-t1)^2));
      side2=2;
      xpo=xpo;
      ypo=ypo;
      %pause
    end
  end
  if(sid==3)
    if(least(4*(gr-2)+3,chek)==xpo)
t0=ring(xpo,ypo+1);
      t1=ring(xpo+1,ypo+1);
      t2=ring(xpo-1,ypo+1);
      ring(xpo,ypo)=t0+sqrt(((hs^2))-.25*((t2-t1)^2));
      valuecorn=t0+sqrt(((hs^2))-.25*((t2-t1)^2));
      side3=3;
      xpo=xpo;
      ypo=ypo;
      %pause
    end
  end
  if(sid==4)
    if(least(4*(gr-2)+4,chek)==ypo)
t0=ring(xpo-1,ypo);
      t1=ring(xpo-1,ypo+1);
      t2=ring(xpo-1,ypo-1);
      ring(xpo,ypo)=t0+sqrt(((hs^2))-.25*((t2-t1)^2));
      valuecorn=t0+sqrt(((hs^2))-.25*((t2-t1)^2));
      side4=4;
```

```
xpo=xpo;
ypo=ypo;
%pause
end
end
end
end
```

### B.2 chmi.m

```
function [valuecent]=chmi(gri)
global ring rm cm post sid inflec cond least
smal=1e37;
for side=1:4
smal=1e37;
   for thu=rm-gri:rm+gri
if(side==1)
   if(ring(thu,cm+gri)<smal)</pre>
smal=ring(thu,cm+gri);
post(gri,side)=thu;
   end
end
if(side==2)
   if(ring(rm-gri,thu)<smal)</pre>
smal=ring(rm-gri,thu);
post(gri,side)=thu;
```

```
end
end
if(side==3)
   if(ring(thu,cm-gri)<smal)</pre>
smal=ring(thu,cm-gri);
post(gri,side)=thu;
   end
end
if(side==4)
   if(ring(rm+gri,thu)<smal)</pre>
smal=ring(rm+gri,thu);
post(gri,side)=thu;
   end
end
   end %for thu
    if(side==1)
    remup=(rm-gri);
    remdo=(rm+gri);
      for thu=post(gri,1):-1:remup+1
   if(ring(thu,cm+gri)>ring(thu-1,cm+gri))
```

```
ind=4*(gri-1)+1;
cond(ind)=cond(ind)+1;
inflec(ind,cond(ind))=thu;
least(ind,cond(ind))=thu-1;
side1U=1;
grid=gri;
%pause
  end
  end
 for thu=post(gri,1):remdo-1
  if(ring(thu,cm+gri)>ring(thu+1,cm+gri))
ind=4*(gri-1)+1;
cond(ind)=cond(ind)+1;
inflec(ind,cond(ind))=thu;
least(ind,cond(ind))=thu+1;
side1D=1;
grid=gri;
%pause
  end
 end
end %closes side=1
```

if(side==2)

```
remlft=(cm-gri);
     remrgt=(cm+gri);
       for thu=post(gri,2):-1:remlft+1
    if(ring(rm-gri,thu)>ring(rm-gri,thu-1))
    thu=thu;
    first=ring(cm-gri,thu);
    second=ring(cm-gri,thu-1);
 ind=4*(gri-1)+2;
 cond(ind)=cond(ind)+1;
 inflec(ind,cond(ind))=thu;
 least(ind,cond(ind))=thu-1;
 side2L=2;
 grid=gri;
 %pause
    end
   end
   for thu=post(gri,2):remrgt-1
    if(ring(rm-gri,thu)>ring(rm-gri,thu+1))
 ind=4*(gri-1)+2;
 cond(ind)=cond(ind)+1;
 inflec(ind,cond(ind))=thu;
least(ind,cond(ind))=thu+1;
side2r=2;
grid=gri;
%pause
```

```
end
  end
end %closes side=2
    if(side==3)
    remup=(rm-gri);
    remdo=(rm+gri);
      for thu=post(gri,3):-1:remup+1
   if(ring(thu,cm-gri)>ring(thu-1,cm-gri))
ind=4*(gri-1)+3;
cond(ind)=cond(ind)+1;
inflec(ind,cond(ind))=thu;
least(ind,cond(ind))=thu-1;
side3U=3;
grid=gri;
%pause
  end
  end
  for thu=post(gri,3):remdo-1
   if(ring(thu,cm-gri)>ring(thu+1,cm-gri))
ind=4*(gri-1)+3;
cond(ind)=cond(ind)+1;
inflec(ind,cond(ind))=thu;
```

```
least(ind,cond(ind))=thu+1;
side3D=3;
grid=gri;
%pause
   end
  end
end %closes side=3
      if(side==4)
    remlft=(cm-gri);
    remrgt=(cm+gri);
      for thu=post(gri,4):-1:remlft+1
   if(ring(rm+gri,thu)>ring(rm+gri,thu-1))
ind=4*(gri-1)+4;
cond(ind)=cond(ind)+1;
inflec(ind,cond(ind))=thu;
least(ind,cond(ind))=thu-1;
side4L=4;
grid=gri;
%pause
   end
  end
  for thu=post(gri,4):remrgt-1
```

```
if(ring(rm+gri,thu)>ring(rm+gri,thu+1))
ind=4*(gri-1)+4;
cond(ind)=cond(ind)+1;
inflec(ind,cond(ind))=thu;
least(ind,cond(ind))=thu+1;
side4R=4;
grid=gri;
%pause
   end
  end
end %closes side=4
end %for side
post;
%pause
valuecent=10; %You know
```

### B.3 middle.m

```
function [valuemid]=middle(t0,t1,t2,xmi,ymi)
global ring sid post hsori calmid rm cm gr hsobs xbeg xfin
ybeg yfin obx oby...
    xsizob ysizob
hs=hsori;
if(xmi>=obx+1)
    if(xmi<=obx+xsizob-1)</pre>
```

### B.4 corner.m

```
function [valuecorn]=corner(t0,t1,t2,xpo,ypo)
global ring sid post hsori calmid rm cm gr hsobs xbeg xfin
ybeg yfin
global obx oby xsizob ysizob inflec cond least
hs=hsori;
if(xpo>=obx+1)
    if(xpo<=obx+xsizob-1)
if(ypo>=oby+1)
if(ypo<=oby+ysizob-1)

hs=hsobs;
end
end
end
end
end
ring(xpo,ypo)=t0+sqrt((2*(hs^2))-((t2-t1)^2));</pre>
```

```
prevrin=t0+sqrt((2*(hs^2))-((t2-t1)^2));
valuecorn=t0+sqrt((2*(hs^2))-((t2-t1)^2));
if(gr>1)
for chek=1:10
        if(sid==1)
  if(least(4*(gr-2)+1,chek)==xpo)
            t0=ring(xpo,ypo-1);
          t1=ring(xpo+1,ypo-1);
          t2=ring(xpo-1,ypo-1);
          ring(xpo,ypo)=t0+sqrt(((hs^2))-.25*((t2-t1)^2));
          valuecorn=t0+sqrt(((hs^2))-.25*((t2-t1)^2));
          side1=1;
          xpo=xpo;
          ypo=ypo;
         %pause
        end
      end
     if(sid==2)
        if(least(4*(gr-2)+2,chek)==ypo)
   t0=ring(xpo+1,ypo);
         t1=ring(xpo+1,ypo+1);
         t2=ring(xpo+1,ypo-1);
         ring(xpo,ypo)=t0+sqrt(((hs^2))-.25*((t2-t1)^2));
         valuecorn=t0+sqrt(((hs^2))-.25*((t2-t1)^2));
         side2=2;
         xpo=xpo;
         ypo=ypo;
         %pause
```

```
end
  end
  if(sid==3)
    if(least(4*(gr-2)+3,chek)==xpo)
t0=ring(xpo,ypo+1);
      t1=ring(xpo+1,ypo+1);
      t2=ring(xpo-1,ypo+1);
      ring(xpo,ypo)=t0+sqrt(((hs^2))-.25*((t2-t1)^2));
      valuecorn=t0+sqrt(((hs^2))-.25*((t2-t1)^2));
      side3=3;
      xpo=xpo;
      ypo=ypo;
      %pause
    end
 end
  if(sid==4)
   if(least(4*(gr-2)+4,chek)==ypo)
t0=ring(xpo-1,ypo);
     t1=ring(xpo-1,ypo+1);
     t2=ring(xpo-1,ypo-1);
      ring(xpo,ypo)=t0+sqrt(((hs^2))-.25*((t2-t1)^2));
      valuecorn=t0+sqrt(((hs^2))-.25*((t2-t1)^2));
      side4=4;
      xpo=xpo;
      ypo=ypo;
      %pause
   end
 end
```

end

end

## **Bibliography**

- [1] H.D Keith and F.J. Padden. J. Appl. Phys, 35:1270-1286, 1964.
- [2] H. D. Keith and Jr. F. J. Padden. Spherulitic crystallization from the melt. ii. influence of fractionation and impurity segregation on the kinetics of crystallization. *Journal of Applied Physics*, 35:1286 – 1296, 1964.
- [3] D. C. Bassett and A. S. Vaughan. *Polymer*, 26:717 725, 1985.
- [4] M. Avrami. Journal of Chemical Physics, 8, 1940.
- [5] Hoffman. J. D. and Lauritzen. J. I. Journal of Research of the National Bureau of Standards, 65, 1961.
- [6] W. W. Mullins and R. F. Sekerka. Stability of a planar interface during solidification of a dilute binary alloy. *Journal of Applied Physics*, 35:444 – 451, 1964.
- [7] W. W. Mullins and R. F. Sekerka. Morphological stability of a particle growing by diffusion or heat flow. *Journal of Applied Physics*, 34:323 329, 1963.
- [8] R. Trivedi and W. Kurz. Morphological stability of a planar interface under rapid solidification conditions. *Acta Metallurgica*, 34:1663 1670, 1986.
- [9] S.R. Coriell et al. Journal of Crystal Growth, 140:139 147, 1994.

- [10] M. E. Glicksman. Fundamentals of Dendritic Growth, volume 1. 1996.
- [11] S. Balijepalli and J. M. Schultz. Incipient instability of growth in blends of polymer melts. *Macromolecules*, 29:2095–2102, 1996.
- [12] A.J.Lovinger and Carl C. Gryte. Model for the shape of polymer spherulites formed in a temperature gradient. *Journal of Applied Physics.*, 47:1999 – 2004, 1976.
- [13] E. E. Wahlstorm. Optical Crystallography. Wiley, New York, 1969.
- [14] Y. Huang and J. Petermann. Spherulite growth of polybutene-1 in a thermal gradient. *Polymer Bull.*, 24:649-656, 1990.
- [15] T.G.Ryan and P.D.Calvert. Diffusion and annealing in crystallizing polymers. *Polymer*, 23:877-883, 1982.
- [16] Calvert P.D. Billingham N.C. and Uzuner A. Studies of diffusion in polymers by ultra-violet microscopy-i. Eur. Polym. Journal, 25(7):839-845, 1989.
- [17] Calvert P.D. Billingham N.C. and Uzuner A. Studies of diffusion in polymers by ultra-violet microscopy-ii. Eur. Polym. Journal, 31:258-264, 1990.
- [18] D. Turnbull and J. C. Fisher. Journal of Chemical Physics, 17:71, 1949.
- [19] R. L. Cormia et al. Journal of Chemical Physics, 37:1333, 1962.
- [20] S. Chew et al. The crystallization kinetics of polyethylene under isothermal and non-isothermal conditions. *Polymer*, 30:874 – 881, 1989.
- [21] R. D. Icenogle. Journal of Polymer Science: Polymer Physics Edition, 23:1369
   1391, 1985.

- [22] G. Eder, H. Janeschitz-Kriegel, and S. Liedauer. Crystallization processes in quiescent and moving polymer melts under heat transfer conditions. *Prog. Polym.* Sci., 15:629-714, 1990.
- [23] F. Bernauer. Gedrillte Kristalle in Forschungen zur Kristalkunde.
- [24] Davis G. T. Hoffman, J. D and Lauritzen J. I. *Treatise on Solid State Chemistry*, volume 3.
- [25] F. P. Price and R. W. Kilb. J. Polym. Sci., 57:395, 1962.
- [26] R. Yamada K. Sasaguri and R. S. Stein. Journal of Applied Physics, 35:3188, 1964.
- [27] Y. Fujiwara. Kolloid Z. Z. Polym., 226:135, 1968
- [28] J. M. Crissman and E. Passaglia. J. Res. Natl. Bur. Stand., Sect. A, 70:225, 1966.
- [29] Jin-Young Jung and Michael M. Chen. 1998.
- [30] W Kurz and D.J. Fischer. Fundamentals of solidification. Trans Tech Publications, Netherlands, 1992.
- [31] R.F. Mehl W.A. Johnson. Trans. Am. Inst. Min. Engrs, 135:416, 1939.
- [32] A.N. Kolmogorov. Izv. Akad. Nauk SSSR Ser. Mat., 1:355, 1937.
- [33] Bernhard Wunderlich. Macromolecular Physics, volume 2. Academic Press New York and London, 1982.
- [34] A. Benard. A model for phase change kinetics in polymer composites with significant fiber surface nucleation. to appear in Acta Mater., 1998.

- [35] A. Benard and S. G. Advani. An analytical model for the spherulitic growth in fiber reinforced polymers. to appear in Journal of Applied Ploymer Science, 1998.
- [36] S.D. Hong T. Yuasa R.J. Tabar, A. Wasiak and R.S. Stein. J. Polym. Sci. Polym. Phys. Ed., 19:49, 1981.
- [37] E. Piorkowska A. Galeski. J. Polym. Sci. Polym. Phys. Ed., 19:731, 1981.
- [38] J.M. Haudlin D. Lefebvre N. Billion, C. Magnet. Colloid Polym. Sci., 272:633, 1994.
- [39] L. Rebenfeld N.A. Mehl. J. Polym. Sci. B., 31:1677, 1993.
- [40] C. Auer G. Hinrichsen Th. Krause, G. Kalinka. J. Appl. Polym. Sci., 51:399, 1994.
- [41] Robert C. Mcowen. Partial Differential Equations. Prentice Hall, 1996.
- [42] M. Biermann G. E. W. Sculze. Journal of Materials Science Letters 12, 12:11, 1993.
- [43] Jaime O. Chua A.J.Lovinger and Carl C. Gryte. Studies on the  $\alpha$  and  $\beta$  forms of isotactic polypropylene by crystallization in a temperature gradient. *Journal of polymer Science*, 15:641 656, 1977.
- [44] S. Swaminarayan Ch. Charbon. Modeling the microstructural evolution of thermoplastic composites. *Materials Science and Engineering*, 1997.
- [45] John Vidale. Bulletin of the Seismological Society of America, 78:2062 2076, 1988.
- [46] J.A.Sethian. Level Set Methods. Cambridge University Press, 1996.

[47] B. Engquist and S. J. Osher. Stable and entropy-satisfying approximations for transonic flow calculations. *Math. Comp*, 34:45, 1980.

